

secretion, and/or resorption by the kidney. All of these conventional markers indirectly estimate kidney function. In contrast, U-L-FABP indicates kidney injury by directly measuring protein levels [10]. Recent studies have shown that U-L-FABP may be a useful marker of acute and progressive renal disease [11,12], however, the clinical significance of U-L-FABP measurement in patients with CAD has not been completely investigated. A recent study demonstrated the clinical benefit of U-L-FABP measurement for the diagnosis of ACS [13], but to date, there are no data evaluating the clinical significance of U-L-FABP measurement in predicting future cardiovascular events in patients with ACS. Therefore, we investigated U-L-FABP levels in patients with ACS, including those with acute myocardial infarction (AMI) and unstable angina pectoris (UAP). In addition, we assessed whether U-L-FABP measurement could identify patients at high risk of future cardiovascular events.

Methods

Study subjects

Fifty consecutive patients (39 male, mean age 64 ± 12 years) with ACS (37 with AMI, and 13 with UAP) who underwent primary percutaneous coronary intervention (PCI) between April 2007 and April 2008 at Juntendo University Hospital were enrolled in this study. Forty seven subjects in an outpatient clinic (33 male, mean age 60 ± 13 years) were included as the control group. Control subjects had no history of CAD and no evidence of coronary ischemia examined by stress cardiac testing. ACS was defined by high-risk UAP, non-ST elevation MI (NSTEMI), or ST elevation MI (STEMI). Electrocardiographic criteria for the diagnosis of STEMI/NSTEMI were as follows: (1) persistent (>20 min) ST elevation in contiguous leads with cut-off points ≥ 0.2 mV in men or ≥ 0.15 mV in women in leads V2–V3 and/or ≥ 0.1 mV in other leads in both sexes; (2) new ST depression horizontal or down-sloping ≥ 0.05 mV in 2 contiguous leads, and/or T inversion ≥ 0.1 mV in two leads in prominent R wave or R/S ratio > 1.3 ; (3) new detection of complete left bundle branch block; and (4) increase (≥ 2 fold) in serum creatine phosphokinase and troponin T positivity. Patients with cardiac shock, acute renal disease, end-stage renal failure requiring dialysis, an estimated GFR (eGFR) < 50 mL/min/1.73 m², hepatic dysfunction, collagen disease, and those using nonsteroidal anti-inflammatory drugs were excluded. None of the control subjects had a history of cardiovascular disorders or systemic inflammatory diseases. The ethical committee of Juntendo University, School of Medicine approved the study protocol and written informed consent was obtained from all subjects.

Analyses of urine and blood samples

Urine samples were collected just before and 24 h after PCI in the ACS group and at the time of clinic visit in the control group. All samples were stored at -20°C until analysis. U-L-FABP levels were measured using a two-step sandwich enzyme-linked immunosorbent assay (CMIC, Tokyo, Japan). Urinary albumin (U-Alb) levels were measured by immunoturbidimetry and adjusted by urinary creatinine (U-Cr). Because U-L-FABP/U-Cr was not normally distributed, the value was expressed as the log-normal distribution of the ratio of U-L-FABP to U-Cr (U-L-FABP/U-Cr). Other serum parameters were measured for all subjects, at the same time urine samples were taken. Serum creatinine, troponin-T, creatinine phosphokinase, high sensitive C-reactive protein (hsCRP), and brain natriuretic protein (BNP) levels were analyzed by standard methods [14]. The eGFR was calculated using the following equation: $\text{eGFR} = 194 \times \text{age}^{-0.287} \times \text{Cr}^{-1.094} \times 0.739$ (if female), according to the Modification of Diet in Renal Disease

Study [15]. Total cholesterol, triglyceride, and high-density lipoprotein cholesterol (HDL-C) levels were also measured by standard methods. Low-density lipoprotein cholesterol levels were calculated by Friedewald's formula. Hemoglobin (Hb) A1c (JDS) (%) was measured as previously described Japanese standard substance and measurement methods and NGSP criteria for measurement of HbA1c.

PCI and antiplatelet therapy

The intervention procedure was performed according to the standard technique of each operator, as previously described [16,17]. The endpoint of the procedure for the main vessel was thrombolysis in myocardial infarction 3 and the absence of major dissections that would compromise flow in the vessel. Intravenous unfractionated heparin was administered before PCI. All patients in the ACS group were implanted with bare-metal stents. Follow-up coronary angiography was performed 6–8 months after stent implantation. A technician without any knowledge of the study results performed all the quantitative coronary angiography (QCA) analyses, as previously described [18]. The absolute values for the mean reference diameter and minimal luminal diameter were determined. Angiographic restenosis was defined as a diameter stenosis $\geq 50\%$ at the follow-up angiography as determined by QCA analysis. Patients in the ACS group received dual antiplatelet therapy of clopidogrel (300 mg loading dose, followed by 75 mg daily) and aspirin (200 mg loading dose and 100 mg daily throughout the study period). All patients in the ACS group were followed for up to 54 months (median 42 months). Major adverse cardiocerebrovascular events (MACCEs) were defined as all-cause death, nonfatal MI, UAP, revascularization for target lesion or new lesion, and admission for stroke.

Statistical analysis

Statistical analysis was performed with Stat View 5.0 MDSU statistical software (SAS Institute, Cary, NC, USA). Data are presented as means \pm standard deviations (SD). Linear regression analysis was used to evaluate the correlation between the 2 variables. $p < 0.05$ was considered statistically significant. Categorical and continuous variables were compared by a *chi*-square analysis. Cox proportional hazard analysis was performed to identify independent predictors for the MACCEs including age, gender, body mass index (BMI), diabetes mellitus, hypertension, dyslipidemia, eGFR, and log (U-L-FABP/U-Cr) levels.

Results

Characteristics of study subjects

Table 1 summarizes the baseline characteristics of each group. There were no significant differences in age, gender, BMI, blood pressure, serum glucose profiles, and eGFR between the ACS and the control groups. Serum BNP and hsCRP levels in the ACS group were significantly higher than those in the control group ($p < 0.005$, $p < 0.05$, respectively). HDL-C levels in the ACS group were significantly lower than those in the control group ($p < 0.005$). The ACS group had significantly higher prevalence of dyslipidemia ($p < 0.005$), metabolic syndrome ($p < 0.005$), and smoking ($p < 0.005$) and significantly higher levels of waist circumference ($p < 0.05$) than the control group. Concomitant use of beta-blockers and statins was more frequent in the ACS group than in the control group ($p < 0.05$, $p < 0.005$, respectively). There were no significant differences in use of angiotensin-converting enzyme inhibitors (ACEIs), angiotensin receptor blockers (ARBs), calcium-channel blockers (CCBs), and anti-diabetic agents between the two groups.

Table 1
Comparison of clinical characteristics between the control and the ACS groups.

	Control	ACS	ACS	
			AMI	UAP
<i>n</i>	47	50	37	13
Age, years	60 ± 13.0	64 ± 11.9	64 ± 12.4	63 ± 11.3
Male (%)	33(70)	39(78)	27(73)	12(92)
Body mass index, kg/m ²	22.7 ± 2.2	23.7 ± 3.5	23.8 ± 3.4	23.4 ± 3.0
Waist circumference, cm	78.2 ± 2.56	87.7 ± 8.9*	88.2 ± 9.4*	87.9 ± 8.3*
Systolic blood pressure, mmHg	129 ± 21	125 ± 21	123 ± 21	128 ± 21
Dyastolic blood pressure, mmHg	71 ± 13	73 ± 13	72 ± 14	74 ± 9
Hypertension (%)	25(53)	31(62)	21(57)	10(77)
Diabetes mellitus (%)	7(15)	14(28)	10(27)	4(31)
Dyslipidemia (%)	11(23)	35(70)**	23(62)**	12(92)**+
Metabolic syndrome (%)	5(11)	18(36)**	12(32)*	6(46)**+
Smoker (%)	5(11)	28(56)**	19(51)**	9(69)**
Estimated GFR, ml/min/1.73 m ²	81.7 ± 26.8	80.2 ± 17.7	79.1 ± 17.0	80.9 ± 7.4
Total cholesterol (mg/dl)	178 ± 38	185 ± 32	188 ± 28	182 ± 38
Triglyceride (mg/dl)	130 ± 32	123 ± 60	122 ± 67	124 ± 41
HDL-cholesterol, mg/dl	51 ± 12	44 ± 11**	43 ± 9**	47 ± 14
LDL-cholesterol, mg/dl	111 ± 32	108 ± 39	112 ± 42	98 ± 24
Blood glucose, mg/dl	105 ± 35	116 ± 38	114 ± 36	117 ± 39
HbA1c, % (JDS)	5.6 ± 0.7	5.6 ± 0.9	5.7 ± 0.8	5.6 ± 1.0
BNP, pg/mL	49 ± 38	294 ± 249**	338 ± 318**	245 ± 114**
hsCRP, mg/dL	0.059 ± 0.039	2.835 ± 1.541*	3.157 ± 1.794*	2.576 ± 1.466*
Ejection fraction, %	(-)	56.9 ± 10.6	55.1 ± 9.4	60.1 ± 13.1
Number of diseased vessels				
One (%)	(-)	24(48)	17(45)	7(55)
Two (%)	(-)	18(36)	16(43)	2(15)
Three (%)	(-)	8(16)	4(11)	4(30)
Use of medication				
ACEI/ARB (%)	25(53)	29(58)	25(68)	4(31)
Beta-blockers (%)	16(34)	27(54)*	21(57)*	6(46)*
Statins (%)	11(23)	33(66)**	26(70)**	7(54)*

Values are mean ± SD.

ACS, acute coronary syndrome; AMI, acute myocardial infarction; UAP, unstable angina pectoris; GFR, glomerular filtration rate; HDL, high-density lipoprotein. LDL, low-density lipoprotein; HbA1c, hemoglobin A1c; JDS, Japan Diabetes Society. BNP, brain natriuretic protein; hsCRP, high sensitive C-reactive protein. ACEI, angiotensin-converting enzyme inhibitors; ARB, angiotensin receptor blockers.

* $p < 0.05$ vs. control.

** $p < 0.005$ vs. control.

+ $p < 0.05$ vs. AMI.

None of the patients who underwent angiography showed contrast medium-induced nephropathy, as defined by Harjai et al. [19].

U-L-FABP levels in the ACS and the control groups

Log (U-L-FABP/U-Cr) levels for each group are shown in Fig. 1. Before angiography, log (U-L-FABP/U-Cr) levels in the ACS group were significantly higher than those in the control group ($p = 0.0024$). In addition, log (U-L-FABP/U-Cr) levels in patients with AMI ($p = 0.0018$), but not in those with UAP, were significantly higher than those in control subjects.

Next, the correlations between log (U-L-FABP/U-Cr) levels and other serum parameters were analyzed. Log (U-L-FABP/U-Cr) levels positively correlated with log BNP levels ($r = 0.323$, $p = 0.001$; Fig. 2A). U-L-FABP levels have been reported to be positively correlated with U-Alb levels [20]. Our data also revealed a positive correlation between log (U-L-FABP/U-Cr) and U-Alb/U-Cr levels ($r = 0.500$, $p < 0.0001$) (Fig. 2B). In addition, no significant correlation was found between log (U-L-FABP/U-Cr) levels and other serum parameters (data not shown). Interestingly, duration of hospitalization was positively correlated with log (U-L-FABP/U-Cr) levels ($r = 0.296$, $p = 0.025$) (Fig. 2C).

Follow-up data in the ACS group

Follow-up angiography was performed in 49 patients (98%). One patient refused angiographic follow-up, because of absence of angina and negative exercise testing. Angiographic in-stent

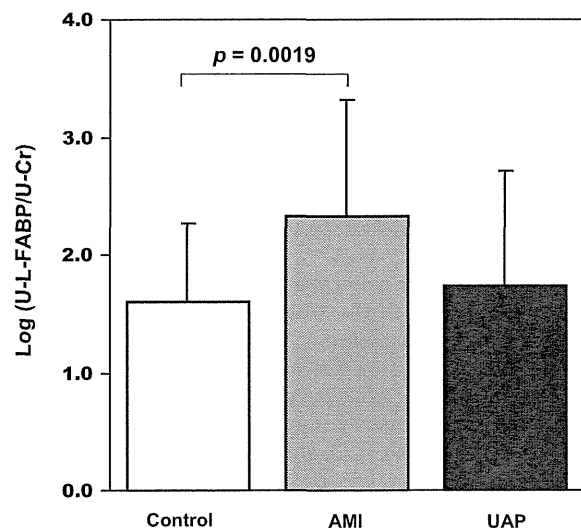


Fig. 1. Comparison of U-L-FABP levels between the ACS (AMI and UAP) and the control groups. Log (U-L-FABP/U-Cr) levels in the ACS group ($n = 50$) were significantly higher than those in the control group ($n = 47$) ($p = 0.0024$). Log (U-L-FABP/U-Cr) levels in patients with AMI ($n = 37$), but not in those with UAP ($n = 13$), were significantly higher ($p = 0.0019$) than those in the control group. ACS, acute coronary syndrome; AMI, acute myocardial infarction; UAP, unstable angina pectoris; U-L-FABP, urinary liver-type fatty acid-binding protein; U-Cr, urinary creatinine.

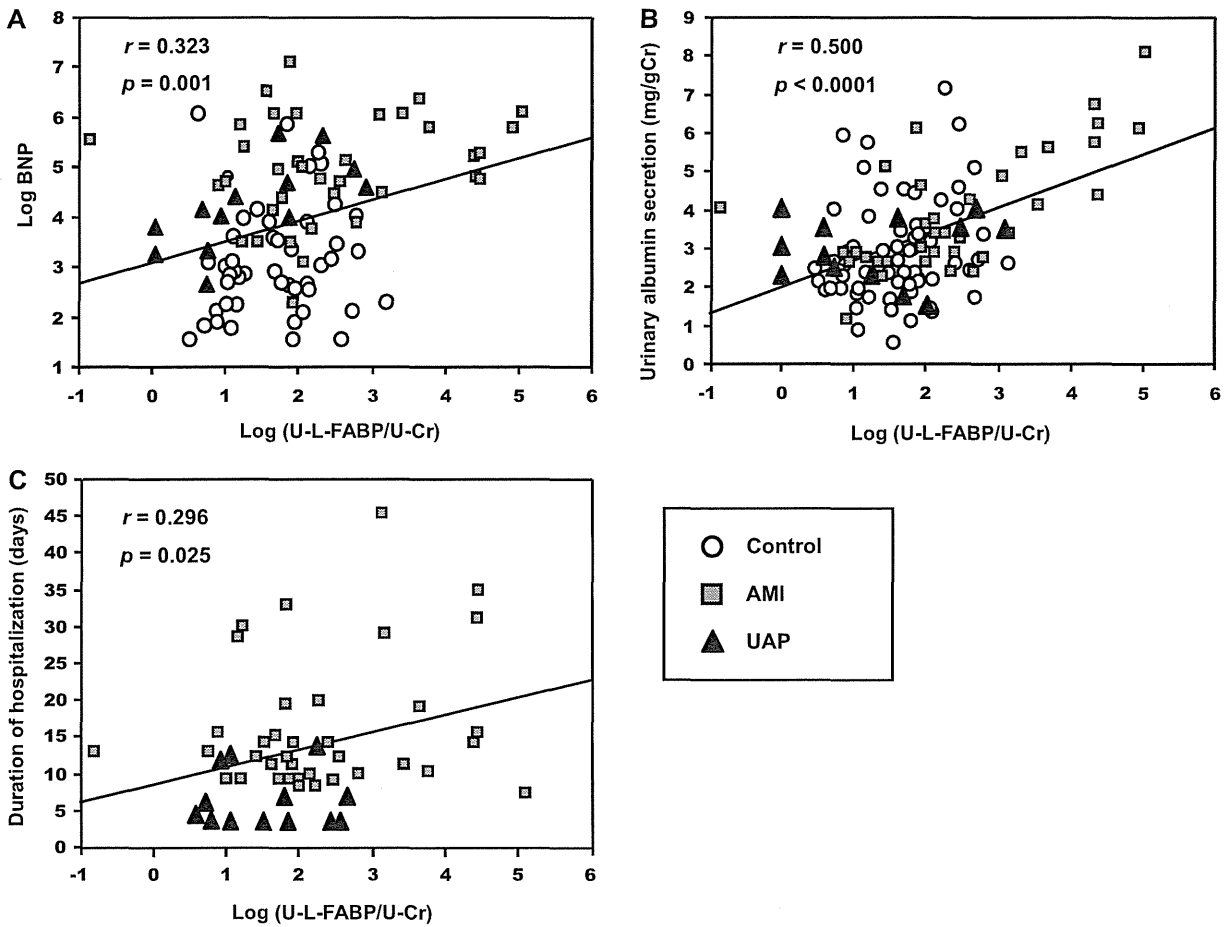


Fig. 2. Correlation between U-L-FABP levels and other parameters. (A) A positive correlation was observed between log (U-L-FABP/U-Cr) and log BNP ($r = 0.323$, $p = 0.001$) ($n = 89$). (B) A positive correlation was observed between log (U-L-FABP/U-Cr) and U-Alb/U-Cr levels ($r = 0.500$, $p < 0.0001$) ($n = 97$). (C) A positive correlation was observed between duration of hospitalization and log (U-L-FABP/U-Cr) levels ($r = 0.296$, $p = 0.025$) ($n = 50$). BNP, brain natriuretic protein; U-L-FABP, urinary liver-type fatty acid-binding protein; U-Cr, urinary creatinine; AMI, acute myocardial infarction; UAP, unstable angina pectoris.

restenosis with ischemic sign evaluated by exercise testing was evident in 4 patients at follow-up angiography. The restenosis (+) group exhibited significantly higher log (U-L-FABP/U-Cr) and U-Alb/U-Cr levels at admission than the restenosis (-) group

($p = 0.047$, $p < 0.0001$, respectively) (Fig. 3A and B). MACCEs were observed in 9 patients (nonfatal MI 1 patient and revascularization 8 patients). At second measurement, log (U-L-FABP/U-Cr) levels in the MACCE (+) group were significantly higher than

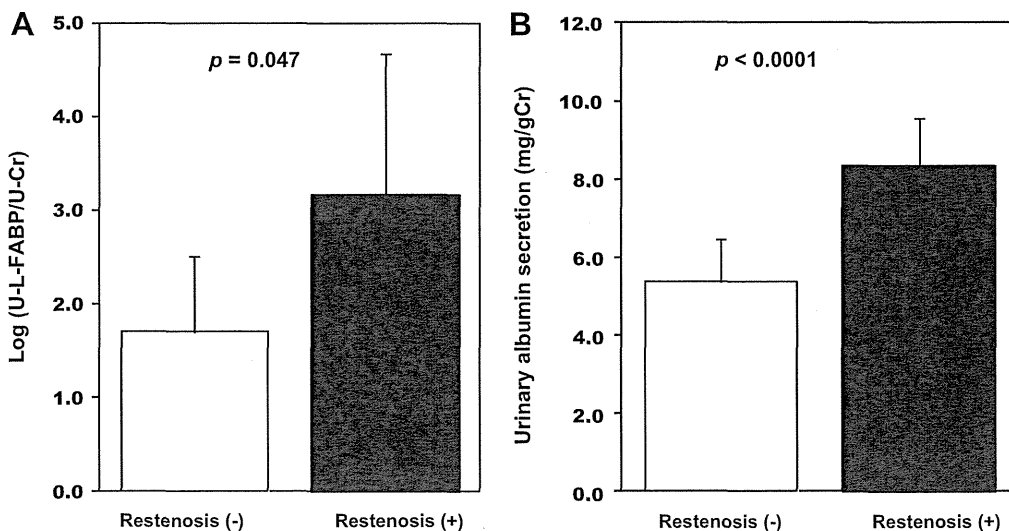


Fig. 3. U-L-FABP and U-Alb levels in patients with and without in-stent restenosis at follow-up angiography. (A) The restenosis (+) group ($n = 4$) exhibited significantly higher log (U-L-FABP/U-Cr) levels than the restenosis (-) group ($p = 0.047$). (B) The restenosis (+) group showed significantly higher U-Alb/U-Cr levels than the restenosis (-) group ($p < 0.0001$). U-L-FABP, urinary liver-type fatty acid-binding protein; U-Cr, urinary creatinine; U-Alb, urinary albumin.

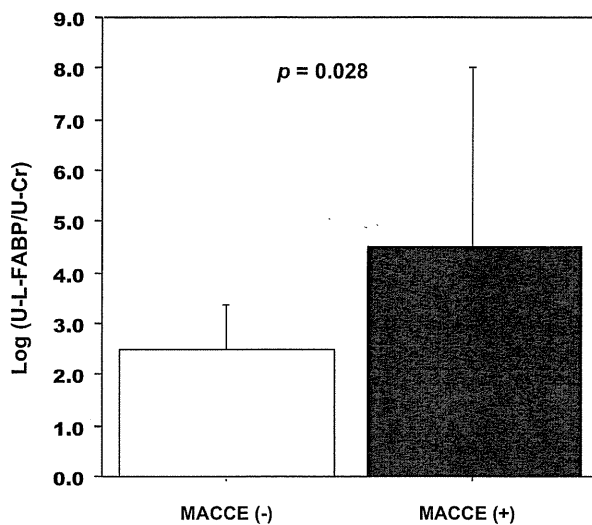


Fig. 4. U-L-FABP levels at second measurement and MACCEs. At second measurement, the MACCEs (+) group ($n=9$) exhibited significantly higher log (U-L-FABP/U-Cr) levels than the MACCEs (-) group ($n=20$) ($p=0.028$). MACCEs, major adverse cardiocerebrovascular events; U-L-FABP, urinary liver-type fatty acid-binding protein; U-Cr, urinary creatinine.

those in the MACCE (-) group ($p=0.028$) (Fig. 4). Meanwhile, log (U-L-FABP/U-Cr) levels at admission were not significantly different between the MACCE (+) and MACCE (-) groups. The levels of eGFR before PCI in the MACCE (+) and MACCE (-) groups were 81.3 ± 15.8 ml/min/ 1.73 m² and 82.9 ± 17.3 ml/min/ 1.73 m², respectively. The levels of eGFR after PCI in the MACCE (+) and MACCE (-) groups were 78.8 ± 14.1 ml/min/ 1.73 m² and 70.8 ± 13.3 ml/min/ 1.73 m², respectively. There was no significant difference in eGFR before and after PCI between the two groups. There were no significant differences in risk factors between the two groups. In addition, there was no difference between these groups regarding the concomitant use of medications, including anti-platelet drugs, beta-blockers, CCBs, ACEIs, ARBs, insulin, peroxisome proliferator-activated receptor (PPAR)- γ agonists, or statins. After adjustment for age, gender, BMI, diabetes mellitus, hypertension, dyslipidemia, and eGFR, multivariate Cox proportional hazard analysis revealed that log (U-L-FABP/U-Cr) levels were significant and independent factors for MACCEs ($p=0.019$).

Discussion

This study demonstrated that U-L-FABP levels in patients with AMI, but not in patients with UAP, were significantly higher than those in the control subjects. In addition, U-L-FABP levels were independent factors for MACCEs in patients with ACS. To the best of our knowledge, this is the first report that demonstrates the significance of U-L-FABP measurement in identifying high-risk subjects among patients with ACS.

The potential reasons why U-L-FABP levels in patients with AMI, but not in patients with UAP, were significantly higher than those in controls should be discussed. Fukuda et al. [13] reported a significant difference in log (U-L-FABP/U-Cr) levels between the ACS group and the stable AP (SAP) groups, and that log (U-L-FABP/U-Cr) may be a useful marker for the diagnosis of ACS. However, the difference in U-L-FABP levels between the AMI and the UAP groups had not been elucidated, because the previous study did not discriminate between AMI and UAP. L-FABP is an intracellular lipid chaperone that selectively binds unsaturated FAs or lipid peroxidation products and transports them to mitochondria or peroxisomes, where they are metabolized by β -oxidation [21]. FAs are important in mammals as mediators of signal transduction for metabolic

regulation and are rarely present in the free state in biological fluids, because of their hydrophobic character and cytotoxicity. Overproduction of FFAs induces oxidative stress and production of inflammatory cytokines by increasing mitochondrial reactive oxygen species, and subsequently leads to tubulointerstitial damage [22]. It is well established that FFA levels are increased in AMI [23] and renal ischemia [24]. Therefore, U-L-FABP levels may be high especially in patients with AMI.

This study also demonstrated the novel findings that U-L-FABP levels at admission positively correlated with BNP levels and duration of hospitalization, and that U-L-FABP levels 24 h after primary PCI were associated with future cardiovascular events. Difference in U-L-FABP and peak CK levels was not statistically significant (Supplement Fig. 1A), however, troponin T levels were positively correlated with U-L-FABP levels in the AMI group (Supplement Fig. 1B). Moreover, positive correlations between U-L-FABP levels, BNP levels, and duration of hospitalization may indicate the extent of cardiac injury, as discussed above. In the follow-up study, the restenosis (+) group showed significantly higher log (U-L-FABP/U-Cr) and U-Alb/U-Cr levels at admission than those in the restenosis (-) group. We evaluated whether the clinical and lesion characteristics could affect the incidence of restenosis between the two groups. The restenosis (+) group included only patients with AMI, and showed higher prevalence of hypertension, dyslipidemia, and current smoking (data not shown). Although lesion characteristics did not show significant difference between the two groups, the difference in clinical characteristics may contribute to an increase in hyperplasia at PCI site, and subsequently lead to restenosis. Further investigations are required to assess these points.

The fact that U-L-FABP levels 24 h after primary PCI, but not at admission, helps in identifying high-risk patients for future cardiovascular events is intriguing. A previous study showed that unbound serum FFAs levels immediately after PCI were 14-fold higher than those before PCI [25]. Moreover, U-L-FABP levels 24 h after PCI remained high in patients with ACS and even in patients with SAP [13]. Increased and/or sustained U-L-FABP levels 24 h after primary PCI may indicate not only oxidative stress and an inflammatory state caused by cardiac injury, but also coronary damage, including at the PCI site. Excessive damage and healing could induce hyperplasia at the PCI site, and subsequently lead to restenosis. In addition, increased oxidative stress accounts for a significant proportion of endothelial dysfunction, which is impaired in CAD, especially in ACS [26]. Endothelial dysfunction and FFA overload may play an important role in the pathogenesis of ACS and increase U-L-FABP levels, although no clear evidence has been reported that characterizes the relationship between cardiac injury and tubulointerstitial injury. Moreover, several lines of evidence indicate that activation of L-FABP in proximal tubules could be triggered not only by overproduction of FFAs, but also by tubular ischemia [27]. Systemic hypoxia caused by ACS induces both renal parenchymal and tubulointerstitial ischemia. Hypoxia is correlated with transcriptional activation of L-FABP because the promoter region of L-FABP contains the binding sites of hepatocyte nuclear factor, hypoxia-inducible factor-1, and PPARs [28].

Despite the novel findings, our study has the following limitations. First, the sample size was small, which limited our ability to determine significance. In addition, second urine samples were obtained 24 h after PCI from 20 (17 patients with AMI and 3 with UAP) of the 41 patients without MACCE. Clinical and angiographic characteristics, including history of AMI and UAP, were not significantly different between the 20 patients from whom second samples were obtained and the 21 patients from whom second samples were not obtained 24 h after PCI. Further investigations with larger sample sizes are needed to clarify our findings and elucidate precise mechanisms. Second, we did not measure U-L-FABP levels during a further follow-up period. Third, U-L-FABP

levels can be affected by treatment with various medications, such as ACEIs or ARBs [29], statins [30], and PPAR γ agonists [31]. However, no significant differences in concomitant use of such medications were observed between the AMI and the UAP groups or between the MACCE (+) and MACCE (–) groups. Finally, we expected that U-L-FABP levels must be increased in patients with contrast medium-induced nephropathy, however, none of the patients who underwent angiography exhibited contrast medium-induced nephropathy.

Conclusions

These results demonstrated that patients with ACS, especially those with AMI, had high U-L-FABP levels, and that urinary L-FABP measurement may help to identify high-risk patients for future cardiovascular events after ACS.

Appendix A. Supplementary data

Supplementary data associated with this article can be found, in the online version, at <http://dx.doi.org/10.1016/j.jcc.2012.03.008>.

References

- [1] Bagshaw SM, Cruz DN, Aspromonte N, Daliento L, Ronco F, Sheinfeld G, Anker SD, Anand I, Bellomo R, Berl T, Bobek I, Davenport A, Haapio M, Hillege H, House A, et al. Epidemiology of cardio-renal syndromes: workgroup statements from the 7th ADQI consensus conference. *Nephrol Dial Transplant* 2010;25:1406–16.
- [2] Ix JH, Shlipak MC, Liu HH, Schiller NB, Whooley MA. Association between renal insufficiency and inducible ischemia in patients with coronary artery disease: the heart and soul study. *J Am Soc Nephrol* 2003;14:3233–8.
- [3] Sarnak MJ, Levey AS, Schoolwerth AC, Coresh J, Culleton B, Hamm LL, McCullough PA, Kasiske BL, Kelepouris E, Klag MJ, Parfrey P, Pfeffer M, Raij L, Spinosa DJ, Wilson PW, et al. Kidney disease as a risk factor for development of cardiovascular disease: a statement from the American Heart Association Councils on Kidney in Cardiovascular Disease, High Blood Pressure Research, Clinical Cardiology, and Epidemiology and Prevention. *Circulation* 2003;108:2154–69.
- [4] Shiba N, Shimokawa H. Chronic kidney disease and heart failure – bidirectional close link and common therapeutic goal. *J Cardiol* 2011;57:8–17.
- [5] Matsuo K, Inoue T, Node K. Estimated glomerular filtration rate as a predictor of secondary outcomes in Japanese patients with coronary artery disease. *J Cardiol* 2009;53:232–9.
- [6] Cruz DN, Bagshaw SM. Heart–kidney interaction: epidemiology of cardio-renal syndromes. *Int J Nephrol* 2010;2011:351291.
- [7] Yamamoto T, Yamamoto A, Watanabe M, Matsuo T, Yamazaki N, Kataoka M, Terada H, Shinohara Y. Classification of FABP isoforms and tissues based on quantitative evaluation of transcript levels of these isoforms in various rat tissues. *Biotechnol Lett* 2009;31:1695–701.
- [8] Maatman RG, van de Westerlo EM, van Kuppevelt TH, Veerkamp JH. Molecular identification of the liver- and the heart-type fatty acid-binding proteins in human and rat kidney. Use of the reverse transcriptase polymerase chain reaction. *Biochem J* 1992;288:285–90.
- [9] Kamijo A, Sugaya T, Hikawa A, Okada M, Okumura F, Yamanouchi M, Honda A, Okabe M, Fujino T, Hirata Y, Omata M, Kaneko R, Fujii H, Fukamizu A, Kimura K. Urinary excretion of fatty acid-binding protein reflects stress overload on the proximal tubules. *Am J Pathol* 2004;165:1243–55.
- [10] Star R, Hostetter T, Hortin GL. New markers for kidney disease. *Clin Chem* 2002;48:1375–6.
- [11] Kamijo A, Kimura K, Sugaya T, Yamanouchi M, Hikawa A, Hirano N, Hirata Y, Goto A, Omata M. Urinary fatty acid-binding protein as a new clinical marker of the progression of chronic renal disease. *J Lab Clin Med* 2004;143:23–30.
- [12] McMahon BA, Murray PT. Urinary liver fatty acid-binding protein: another novel biomarker of acute kidney injury. *Kidney Int* 2010;77:657–9.
- [13] Fukuda Y, Miura S, Zhang B, Iwata A, Kawamura A, Nishikawa H, Shirai K, Saku K. Significance of urinary liver-fatty acid-binding protein in cardiac catheterization in patients with coronary artery disease. *Inter Med* 2009;48:1731–7.
- [14] Hiki M, Shimada K, Ohmura H, Kiyonagi T, Kume A, Sumiyoshi K, Fukao K, Inoue N, Mokuno H, Miyazaki T, Daida H. Serum levels of remnant lipoprotein cholesterol and oxidized low-density lipoprotein in patients with coronary artery disease. *J Cardiol* 2009;53:108–16.
- [15] Matsuo S, Imai E, Horio M, Yasuda Y, Tomita K, Nitta K, Yamagata K, Tomino Y, Yokoyama H, Hishida A. Collaborators developing the Japanese equation for estimated GFR. Revised equations for estimated GFR from serum creatinine in Japan. *Am J Kidney Dis* 2009;53:982–92.
- [16] Okazaki S, Yokoyama T, Miyauchi K, Shimada K, Kurata T, Sato H, Daida H. Early statin treatment in patients with acute coronary syndrome: demonstration of the beneficial effect on atherosclerotic lesions by serial volumetric intravascular ultrasound analysis during half a year after coronary event: the ESTABLISH Study. *Circulation* 2004;110:1061–8.
- [17] Masaki Y, Shimada K, Kojima T, Miyauchi K, Inoue K, Kiyonagi T, Hiki M, Fukao K, Hirose K, Ohsaka H, Kume A, Miyazaki T, Ohmura H, Ohsaka A, Daida H. Clinical significance of the measurements of plasma N-terminal pro-B-type natriuretic peptide levels in patients with coronary artery disease who have undergone elective drug-eluting stent implantation. *J Cardiol* 2011;57:303–10.
- [18] Miyazaki T, Shimada K, Miyauchi K, Kume A, Tanimoto K, Kiyonagi T, Sumiyoshi K, Hiki M, Mokuno H, Okazaki S, Sato H, Kurata T, Daida H. Effects of fenofibrate on lipid profiles, cholesterol ester transfer activity, and in-stent intimal hyperplasia in patients after elective coronary stenting. *Lipids Health Dis* 2010;9:122.
- [19] Harjai KJ, Raizada A, Shenoy C, Sattur S, Orshaw P, Yaeger K, Boura J, Aboufares A, Sporn D, Stapleton D. A comparison of contemporary definitions of contrast nephropathy in patients undergoing percutaneous coronary intervention and a proposal for a novel nephropathy grading system. *Am J Cardiol* 2008;101:812–9.
- [20] Kamijo-Ikemori A, Sugaya T, Yasuda T, Kawata T, Ota A, Tatsunami S, Kaise R, Ishimitsu T, Tanaka Y, Kimura K. Clinical significance of urinary liver-type fatty acid-binding protein in diabetic nephropathy of type 2 diabetic patients. *Diabetes Care* 2011;34:691–6.
- [21] Veerkamp JH, Peeters RA, Maatman RG. Structural and functional features of different types of cytoplasmic fatty acid-binding proteins. *Biochim Biophys Acta* 1991;1081:1–24.
- [22] Sasaki H, Kamijo-Ikemori A, Sugaya T, Yamashita K, Yokoyama T, Koike J, Sato T, Yasuda T, Kimura K. Urinary fatty acids and liver-type fatty acid binding protein in diabetic nephropathy. *Nephron Clin Pract* 2009;112:148–56.
- [23] Oliver MF, Opie LH. Effects of glucose and fatty acids on myocardial ischemia and arrhythmias. *Lancet* 1994;343:155–8.
- [24] Matthys E, Patel Y, Kreisberg J, Stewart JH, Venkatachalam M. Lipid alterations induced by renal ischemia: pathogenic factor in membrane damage. *Kidney Int* 1984;26:153–61.
- [25] Cantor WJ, Kim HH, Jolly S, Moe G, Burstein JM, Mendelsohn A, Kleinfeld AM, Fitchett D. B-type natriuretic peptide and serum unbound free fatty acid levels after contemporary percutaneous coronary intervention. *J Invasive Cardiol* 2008;20:186–8.
- [26] Guarda E, Godoy I, Foncea R, Pérez DD, Romero C, Venegas R, Leighton F. Red wine reduces oxidative stress in patients with acute coronary syndrome. *Int J Cardiol* 2005;104:35–8.
- [27] Yamamoto T, Noiri E, Ono Y, Doi K, Negishi K, Kamijo A, Kimura K, Fujita T, Kinukawa T, Taniguchi H, Nakamura K, Goto M, Shinozaki N, Ohshima S, Sugaya T. Renal L-type fatty acid-binding protein in acute ischemic injury. *J Am Soc Nephrol* 2007;18:2894–902.
- [28] Noiri E, Doi K, Negishi K, Tanaka T, Hamasaki Y, Fujita T, Portilla D, Sugaya T. Urinary fatty acid-binding protein 1: an early predictive biomarker of kidney injury. *Am J Physiol Renal Physiol* 2009;296:669–79.
- [29] Nakamura T, Inoue T, Sugaya T, Kawagoe Y, Suzuki T, Ueda Y, Koide H, Node K. Beneficial effects of olmesartan and temocapril on urinary liver-type fatty acid-binding protein levels in normotensive patients with immunoglobulin A nephropathy. *Am J Hypertens* 2007;20:1195–201.
- [30] Nakamura T, Sugaya T, Kawagoe Y, Ueda Y, Osada S, Koide H. Effect of pitavastatin on urinary liver-type fatty acid-binding protein levels in patients with early diabetic nephropathy. *Diabetes Care* 2005;28:2728–32.
- [31] Nakamura T, Sugaya T, Kawagoe Y, Ueda Y, Koide H. Effect of pioglitazone on urinary liver-type fatty acid-binding protein concentrations in diabetes patients with microalbuminuria. *Diabetes Metab Res Rev* 2006;22:385–9.

Post-prandial remnant lipoprotein metabolism in autosomal recessive hypercholesterolaemia

Hayato Tada*, Masa-aki Kawashiri*, Akira Tanaka[†], Takamitsu Nakano[‡], Katsuyuki Nakajima[‡], Takeshi Inoue*, Tohru Noguchi[§], Chiaki Nakanishi*, Tetsuo Konno*, Kenshi Hayashi*, Atsushi Nohara[§], Akihiro Inazu[¶], Junji Kobayashi[§], Hiroshi Mabuchi[§] and Masakazu Yamagishi*

*Division of Cardiovascular Medicine Kanazawa University Graduate School of Medicine, Kanazawa, Japan, [†]Nutrition Clinic, Kagawa Nutrition University, Sakado, Japan, [‡]School of Health Sciences, Faculty of Medicine, Gunma University, Maebashi, Japan, [§]Department of Lipidology, Graduate School of Medical Science, Kanazawa University, Kanazawa, Japan, [¶]Department of Laboratory Science, Graduate School of Medical Science, Kanazawa University, Kanazawa, Japan

ABSTRACT

Background Phenotype of autosomal recessive hypercholesterolaemia (ARH), a rare lipid disorder, is known to be milder than that of homozygous familial hypercholesterolaemia (FH) with LDL receptor gene mutation. However, few data exist regarding the functional differences in ARH and FH particularly in terms of remnant-like particles' (RLP) metabolism.

Materials and methods Blood sampling was performed up to 6 h after OFTT cream loading (50 g/body surface area) with 2-h intervals in a single ARH proband, four heterozygous FH patients with LDL receptor gene mutation and four normal controls. Plasma lipoprotein and RLP fraction were determined by HPLC system. The area under curve (AUC) of each lipoprotein including RLP fractions was evaluated.

Results The AUC of TG, RLP cholesterol (RLP-C) and RLP triglyceride (RLP-TG) levels of heterozygous FH subjects was significantly higher than those of controls (466 ± 71 mg/dL \times h vs. 303 ± 111 mg/dL \times h, $P < 0.05$; 35 ± 7 mg/dL \times h vs. 21 ± 8 mg/dL \times h, $P < 0.05$; 124 ± 57 mg/dL \times h vs. 51 ± 13 mg/dL \times h, $P < 0.05$, respectively). Under these conditions, those values of ARH were close to those of controls (310 mg/dL \times h, 22 mg/dL \times h, 23 mg/dL \times h, respectively).

Conclusion These data demonstrate that unlike in FH, RLP clearance is preserved in ARH. The preservation of post-prandial RLP clearance may contribute to the mild phenotype of ARH compared with FH.

Keywords Autosomal recessive hypercholesterolaemia, familial hypercholesterolaemia, LDLR adaptor protein 1, oral fat tolerance test, remnant-like-particles.

Eur J Clin Invest 2012; 42 (10): 1094–1099

Introduction

Familial hypercholesterolaemia (FH) is a common inherited disorder of plasma lipoprotein metabolism, characterized by an elevated level of LDL cholesterol (LDL-C), tendon xanthomas and premature coronary artery disease [1]. Genetic causes of FH involve gene mutations such as LDL receptor (LDLR), apolipoprotein B-100 (apoB100) and proprotein convertase subtilisin/kexin type 9 (PCSK9) [2]. Recently, post-prandial accumulation of lipoprotein remnants has been shown to be related with elevated cardiovascular risk [3]. As for FH, it has been shown that post-prandial lipoprotein metabolism is also severely impaired [4].

Autosomal recessive hypercholesterolaemia (ARH), the cause of which is a mutation in LDLR adaptor protein 1 (LDLRAP1) gene, is an extremely rare disorder resembling FH [5]. However, the clinical manifestations of ARH such as plasma LDL-C levels seem to be between heterozygous and homozygous FH, and lipid-lowering therapy including statin is effective [6–9]. Although this advantage has been explained partially for the preservation of VLDL remnant clearance in LDLRAP1 knockout mice (ARH mice) [10], the rarity of this disease makes it difficult to understand the lipoprotein metabolism, especially post-prandial metabolism of remnant-like

particles (RLP) in human ARH patient. Recently, we demonstrated that the clearance of VLDL remnant is paradoxically accelerated in ARH patient by kinetic study using stable isotope [11]. In this study, we examined post-prandial lipoprotein metabolism in ARH in terms of differences from that in FH as well as normal controls.

Materials and methods

Study subjects

We enrolled an ARH patient, whose clinical phenotype was described elsewhere [11]. To compare post-prandial remnant lipoprotein levels, FH patients with single LDLR gene mutation (c.2431A>T, previously described as K790X) and healthy normal subjects were also enrolled. Because glucose tolerability and apolipoprotein E isoform may affect the remnant lipoprotein levels, subjects with diabetes mellitus and apoE isoform other than E3/2 were excluded. All study subjects were male. Written informed consent was obtained from all the study subjects to participate in the study. None of the subjects had taken medication known to affect plasma lipids for at least 4 weeks before this study conducted. None had smoking habits and excessive alcohol intake (> ethanol 40 g/day).

Oral fat tolerance test (OFTT)

Oral fat tolerance test cream of 50 g was given per body surface area (m²) as described in elsewhere (Jomo Shokuhin, Takasaki, Japan) [12]. The cream consisted of fat 33%, cholesterol 74 mg and 341 kcal per 100 g, rich in palmitic and oleic acids. Blood sampling was performed at 2-h intervals up to 6 h.

Lipoprotein analysis and apoE phenotype

RLP is estimated as the unbound fraction of plasma after incubation with immunoaffinity gel of apoB100 monoclonal antibody and apolipoprotein A-I monoclonal antibody as described [13]. Plasma lipoprotein and RLP cholesterol distribution was determined by HPLC system using two tandem connected TSK gel Lipopropak XL columns and 0.05 M Tris-buffered acetate (pH 8.0) at a flow rate of 0.7 mL/min (Tosoh, Tokyo, Japan) as described [14]. ApoE phenotype was separated by isoelectric focusing and detected by western blot with apoE polyclonal antibody (phenotyping apoE IEF system, JOKOH, Tokyo, Japan). Apolipoprotein B-48 (apoB48) levels were determined by ELISA method using monoclonal antibody against C-terminal decapeptide of apoB48 [15].

Statistical analysis

Values are expressed as mean \pm SD unless otherwise stated. Area under curve (AUC) for triglyceride (TG), RLP triglyceride (RLP-TG), RLP cholesterol (RLP-C) and apoB48 levels at baseline and after fat load was calculated using trapezoid rule.

Differences of changes were compared with unpaired *t*-test. Fisher's exact test was used for comparing proportions between FH patients and normal controls. The level of statistical significance was set at $P < /0.05$. Statistical analysis was performed using STATVIEW 5.0 (SAS Institute Japan, Tokyo, Japan).

Results

The baseline characteristics of the three study groups are shown in Table 1. These groups of patients were comparable in terms of age, gender and body mass index (BMI). Furthermore, the apoE phenotype of all the study subjects was apoE3/2. The baseline lipid levels of ARH patient were similar to those of FH patients. FH patients showed significantly higher fasting plasma total cholesterol (TC) and LDL-C concentrations than those of control subjects. However, there were no statistical differences in TG, RLP-C and RLP-TG levels between FH patients and normal controls at the baseline.

As shown in Fig. 1, TG, RLP-C and RLP-TG levels became much higher in heterozygous FH group compared with that of normal control group after oral fat load and returned to the baseline levels after 6 h. In contrast, those lipoprotein fractions of ARH were close to those of normal controls. The AUC of TG, RLP-C and RLP-TG levels of heterozygous FH patients was significantly greater than those of controls (466 ± 71 mg/dL \times h vs. 303 ± 111 mg/dL \times h, $P < 0.05$; 35 ± 7 mg/dL \times h vs. 21 ± 8 mg/dL \times h, $P < 0.05$; 124 ± 57 mg/dL \times h vs. 51 ± 13 mg/dL \times h, $P < 0.05$, respectively, Fig. 2). In contrast, the AUC of TG, RLP-C and RLP-TG levels of ARH was similar with those of normal control subjects

Table 1 Baseline characteristics of the study subjects

	ARH (n = 1)	Heterozygous FH (n = 4)	Normal controls (n = 4)
Age (years)	68	58 \pm 17	62 \pm 17
BMI (kg/m ²)	26.2	23.5 \pm 2.3	23.8 \pm 2.0
TC (mg/dL)	378	316 \pm 50*	173 \pm 44
TG (mg/dL)	66	95 \pm 19	79 \pm 45
LDL-C (mg/dL)	286	241 \pm 26**	88 \pm 6
HDL-C (mg/dL)	45	50 \pm 12	66 \pm 21
RLP-C (mg/dL)	6.1	7.4 \pm 2.7	5.0 \pm 3.0
RLP-TG (mg/dL)	1.5	10.1 \pm 7.4	7.3 \pm 2.4

BMI, body mass index; TC, total cholesterol; TG, triglyceride; LDL-C, low-density lipoprotein cholesterol; HDL, high-density lipoprotein; RLP-C, remnant-like particle cholesterol; RLP-TG, remnant-like particle triglyceride. Values are mean \pm SD; Student's *t*-test was used to compare mean values between heterozygous FH subjects and normal controls.

* $P < 0.05$, ** $P < 0.0001$.

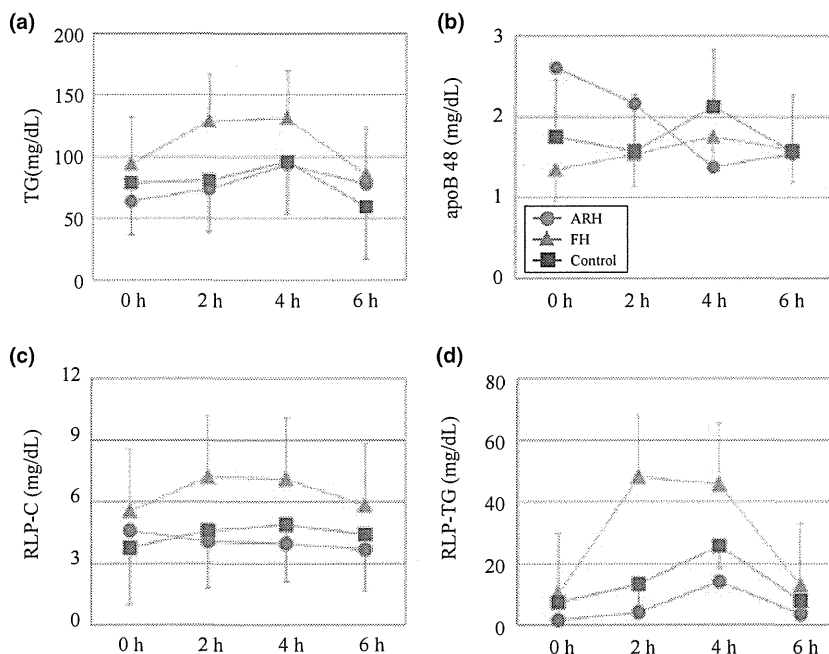


Figure 1 Plasma levels of each lipoprotein after oral fat load. Pink circles indicate ARH; green triangles indicate heterozygous FH; blue squares indicate controls. (a) TG, (b) apoB48, (c) RLP-C, (d) RLP-TG. ARH, autosomal recessive hypercholesterolaemia; FH, familial hypercholesterolaemia; RLP-C, remnant-like particle cholesterol; RLP-TG, remnant-like particle triglyceride; TG, triglyceride.

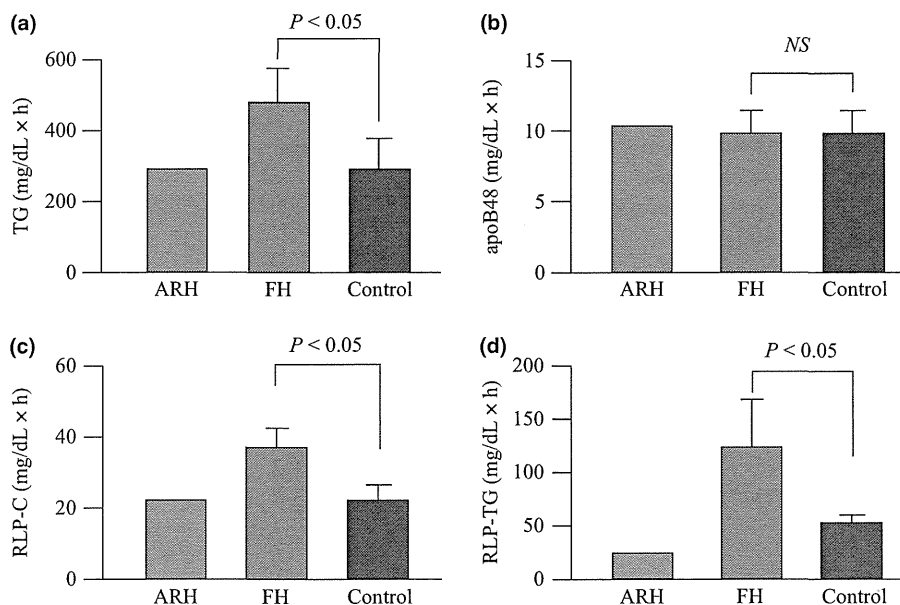


Figure 2 The AUC of each lipoprotein. Pink bars indicate ARH; green bars indicate heterozygous FH; blue bars indicate controls. (a) TG, (b) apoB48, (c) RLP-C, (d) RLP-TG. AUC, area under curve; ARH, autosomal recessive hypercholesterolaemia; FH, familial hypercholesterolaemia; TG, triglyceride; RLP-C, remnant-like particle cholesterol; RLP-TG, remnant-like particle triglyceride.

(310 mg/dL × h, 22 mg/dL × h, 23 mg/dL × h, respectively, Fig. 2).

There was no significant difference observed in the AUC of apoB48 level among those three groups, suggesting that the ability of absorption from intestine was not disturbed in all groups (Fig. 2).

From the HPLC analysis, the formation of chylomicron and chylomicron remnants also seemed to be diminished in the ARH patient in contrast to other study subjects including normal controls (Fig. 3).

Discussion

The main finding of this study is that the clearance of post-prandial RLP was preserved in ARH in contradiction to FH

under the condition of the absence of LDLRAP1. This is the first study to demonstrate the preserved post-prandial lipoprotein metabolism in ARH patient.

In the experimental study using LDLRAP1 knockout mice (ARH mice), cholesterol and TG response on a high-sucrose diet was milder than those in LDLR knockout mice. This is explained for the preservation of VLDL and VLDL remnants clearance of ARH mice [10]. However, few data exist regarding the remnant lipoprotein metabolism of ARH during post-prandial state especially in clinical settings. Previously, we demonstrated that the clearance of VLDL remnant is paradoxically accelerated in ARH patient by kinetic study using stable isotope [11]. However, it is not clear whether the differences in

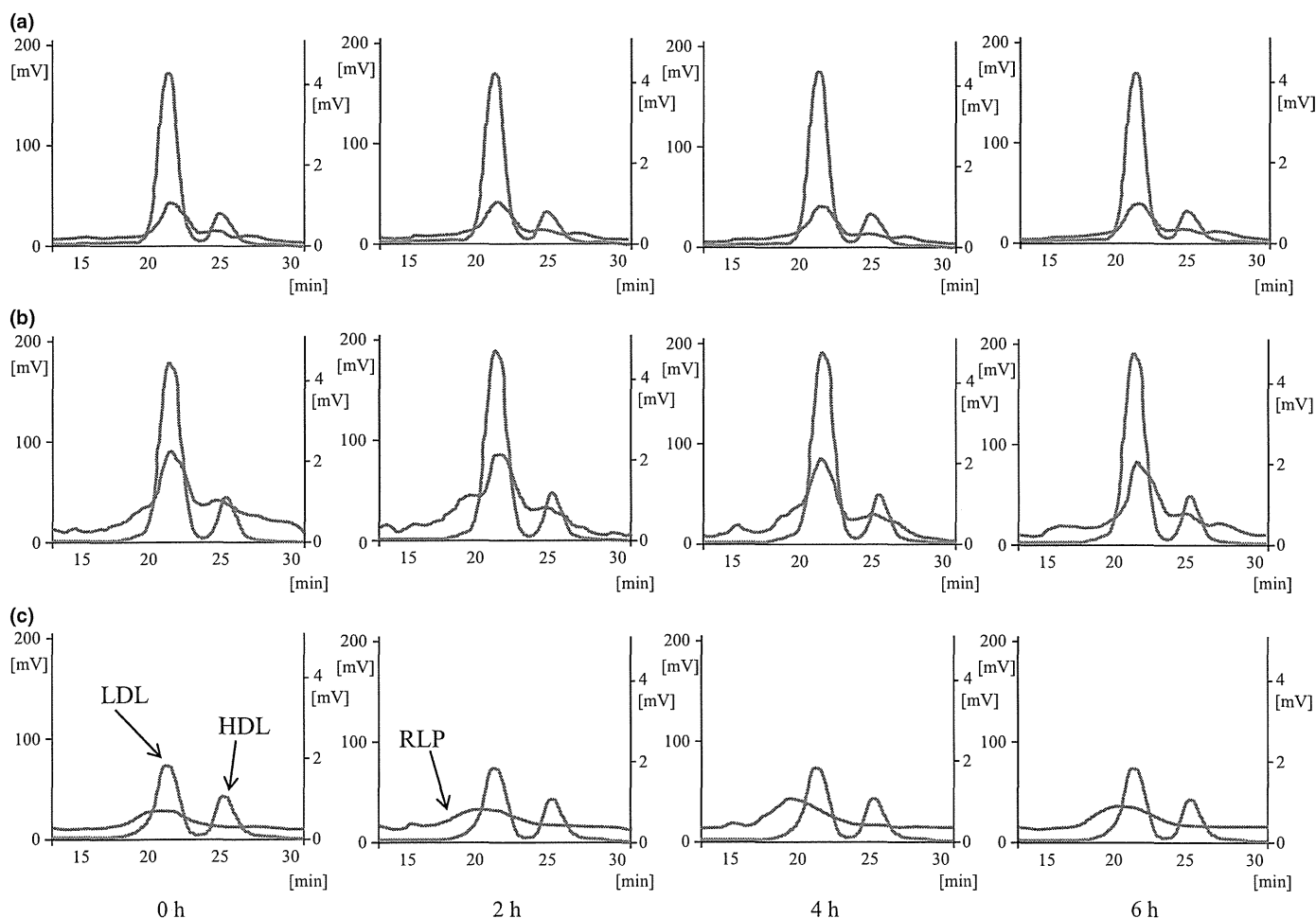


Figure 3 HPLC analysis for representative cases. Cholesterol levels of plasma and RLP fraction by HPLC analysis were shown in red lines and blue lines, respectively. The left peak indicates the LDL fraction, and the right indicates the HDL fraction. The subfraction eluted around 15 min by red line after oral fat load indicates chylomicron and its remnant. (a) ARH, (b) heterozygous FH, (c) normal control. ARH, autosomal recessive hypercholesterolaemia; FH, familial hypercholesterolaemia; HDL, high-density lipoprotein; LDL-C, low-density lipoprotein; RLP, remnant-like particles.

post-prandial lipid levels come not only from endogenous but also from exogenous lipid metabolism.

Chylomicron remnant appears to be catabolized both by the LDLR and LDLR-related protein (LRP), both of which can be compensated in the absence of each receptor. Thus, whether the absence of LDLR affects the metabolism of chylomicron remnants is still controversial [16,17]. However, the metabolism of at least smaller fraction of chylomicron remnants ($S_f < 1000$) depends to some extent on LDLR [18–21]. The ARH patient showed lower chylomicron and chylomicron remnants levels in both fasting and post-prandial state than FH patients. From these considerations, it is assumed that both LDLR and LRP participate in the metabolism of chylomicron remnant and that catabolism of chylomicron remnant through LDLR is not disturbed in the absence of LDLRAP1 protein. The FDNPVY sequence of LDLR binds to the clathrin adaptor proteins, such as LDLRAP1, and facilitates the internalization of ligand [22], but LDLR seems to also have a FDNPVY-independent internalization mechanism [23]. ARH patients may catabolize such RLPs via this alternative pathway that does not need LDLRAP1 protein. In addition to providing new insights into the role of LDLRAP1 in the metabolism of remnant lipoprotein, our results demonstrated that the mutation with internalization defective allele in LDLR (c.2431A>T, previously described as K790X) also could cause the disturbance of remnant lipoprotein metabolism.

Another finding obtained from this study is that the concentration of apoB48 decreased after the fat load in ARH. The possible speculation for this is the involvement of LDLRAP1 in the chylomicron absorption from the intestine, although the expression of LDLRAP1 in human intestine has been reported to be relatively low.

This study has several limitations. First, relatively small number of subjects was included in this study. It is difficult to enrol more ARH patients because of the rarity of this disorder, limiting the statistical analysis for the ARH patient. However, our subjects were comparatively uniform in terms of factors potentially affecting the post-prandial lipoprotein metabolism—there were no statistically significant differences in age and BMI among study subjects. Furthermore, all of the study subjects without diabetes showed apoE3/2 phenotype. We believe that this study of a single ARH patient provides new insights into the roles of LDLRAP1 in the post-prandial lipoprotein metabolism.

Acknowledgements

We express our special thanks to Kazuko Honda and Sachio Yamamoto (staff of Kanazawa University) for their outstanding technical assistance. The authors have nothing to disclose.

Sources of funding

This work has been supported by a scientific research grant from the Ministry of Education, Science, and Culture of Japan (No.21591160), a grant from the Mitsubishi Pharma Research Foundation and Japan Heart Foundation & Astellas / Pfizer Grant for Research on Atherosclerosis Update.

Contributions

Hayato Tada designed the research and preformed research and wrote paper. Masa-aki Kawashiri and Masakazu Yamagishi designed the research and wrote paper. Takamitsu Nakano and Katsuyuki Nakajima designed the research and preformed the research. Akira Tanaka, Takeshi Inoue, Tohru Noguchi, Chiaki Nakanishi, Tetsuo Konno, Kenshi Hayashi, Atsushi Nohara, Akihiro Inazu, Junji Kobayashi and Hiroshi Mabuchi collected the data.

Address

Division of Cardiovascular Medicine Kanazawa University Graduate School of Medicine, 13-1 Takara-machi, Kanazawa 920-8641, Japan (H. Tada, M.-a. Kawashiri, T. Inoue, C. Nakanishi, T. Konno, K. Hayashi, M. Yamagishi); Nutrition Clinic, Kagawa Nutrition University, 3-9-21 Chiyoda, Sakado 350-0288, Japan (A. Tanaka); School of Health Sciences, Faculty of Medicine, Gunma University, 3-39-22 Showa-machi, Maebashi 371-8511, Japan (T. Nakano, K. Nakajima); Department of Lipidology, Graduate School of Medical Science, Kanazawa University, 13-1 Takara-machi, Kanazawa 920-8641, Japan (T. Noguchi, A. Nohara, J. Kobayashi, H. Mabuchi); Department of Laboratory Science, Graduate School of Medical Science, Kanazawa University, 13-1 Takara-machi, Kanazawa 920-8641, Japan (A. Inazu).

Correspondence to: Hayato Tada, Division of Cardiovascular Medicine, Kanazawa University Graduate School of Medicine, 13-1 Takara-machi, Kanazawa 920-8641, Japan. Tel.: +81 76 265 2000 (2251); fax: +81 76 234 4251; e-mail: ht240z@sa3.so-net.ne.jp

Received 15 February 2012; accepted 17 May 2012

References

- Goldstein JL, Hobbs HH, Brown MS. Familial hypercholesterolemia. In: Scriver CR, Beaudet AL, Sly WS, Valle D, editors. *The Metabolic and Molecular Bases of Inherited Diseases*, 8th edn. New York: McGraw-Hill; 2001: pp 2863–913.
- Soutar AK, Naoumova RP. Mechanisms of disease: genetic causes of familial hypercholesterolemia. *Nat Pract Cardiovasc Med* 2007;4:214–25.
- Karpe F, Steiner G, Uffelman K, Olivecrona T, Hamsten A. Post-prandial lipoproteins and progression of coronary atherosclerosis. *Atherosclerosis* 1994;106:83–97.
- de Sauvage Nolting PR, Twickler MB, Dallings-Thie GM, Buirma RJ, Hutten BA, Kastelein JJ *et al*. Elevated remnant-like particles in

- heterozygous familial hypercholesterolemia and response to statin therapy. *Circulation* 2002;106:788–92.
- 5 Harada-Shiba M, Takagi A, Miyamoto Y, Tsushima M, Ikeda Y, Yokoyama S *et al*. Clinical features and genetic analysis of autosomal recessive hypercholesterolemia. *J Clin Endocrinol Metab* 2003;88:2541–7.
 - 6 Soutar AK, Naoumova RP, Traub LM. Genetics, clinical phenotype, and molecular cell biology of autosomal recessive hypercholesterolemia. *Arterioscler Thromb Vasc Biol* 2003;23:1963–70.
 - 7 Pisciotta L, Oliva CP, Pes GM, Di Scala L, Bellocchio A, Fresa R *et al*. Autosomal recessive hypercholesterolemia (ARH) and homozygous familial hypercholesterolemia (FH): a phenotypic comparison. *Atherosclerosis* 2004;188:398–405.
 - 8 Soutar AK, Naoumova RP. Autosomal recessive hypercholesterolemia. *Semin Vasc Med* 2004;4:241–8.
 - 9 Tada H, Kawashiri MA, Ohtani R, Noguchi T, Nakanishi C, Konno T *et al*. A novel type of familial hypercholesterolemia: double heterozygous mutations in LDL receptor and LDL receptor adaptor protein 1 gene. *Atherosclerosis* 2011;219:663–6.
 - 10 Jones C, Garuti R, Michaely P, Li WP, Maeda N, Cohen JC *et al*. Disruption of LDL but not VLDL clearance in autosomal recessive hypercholesterolemia. *J Clin Invest* 2007;117:165–74.
 - 11 Tada H, Kawashiri MA, Ikewaki K, Terao Y, Noguchi T, Nakanishi C *et al*. Altered metabolism of low-density lipoprotein and very low-density lipoprotein remnant in autosomal recessive hypercholesterolemia: evidence from stable isotope kinetic study *in vivo*. *Circ Cardiovasc Genet* 2012;5:35–41.
 - 12 Inazu A, Nakajima K, Nakano T, Niimi M, Kawashiri MA, Nohara A *et al*. Decreased post-prandial triglyceride response and diminished remnant lipoprotein formation in cholesteryl ester transfer protein (CETP) deficiency. *Atherosclerosis* 2008;196:953–7.
 - 13 Nakajima K, Saito T, Tamura A, Suzuki M, Nakano T, Adachi M *et al*. Cholesterol in remnant-like lipoproteins in human serum using monoclonal anti apo B-100 and anti apo A-I immunoaffinity mixed gels. *Clin Chim Acta* 1993;223:53–71.
 - 14 Usui S, Hara Y, Hosaki S, Okazaki M. A new on-line dual enzymatic method for simultaneous quantification of cholesterol and triglycerides in lipoproteins by HPLC. *J Lipid Res* 2002;43:805–14.
 - 15 Kinoshita M, Kojima M, Matsushima T, Teramoto T. Determination of apolipoprotein B-48 in serum by a sandwich ELISA. *Clin Chim Acta* 2005;351:115–20.
 - 16 Choi SY, Fong LG, Kirven MJ, Cooper AD. Use of an anti-low density lipoprotein receptor antibody to quantify the role of the LDL receptor in the removal of chylomicron remnants in the mouse *in vivo*. *J Clin Invest* 1991;88:1173–81.
 - 17 Ishibashi S, Perrey S, Chen Z, Osuga J, Shimada M, Ohashi K *et al*. Role of the Low Density Lipoprotein (LDL) receptor pathway in the metabolism of chylomicron remnants. *J Biol Chem* 1996;271:22422–7.
 - 18 Cabezas MC, de Bruin TW, Westerveld HE, Meijer E, Erkelens DW. Delayed chylomicron remnant clearance in subjects with heterozygous familial hypercholesterolaemia. *J Intern Med* 1998;244:299–307.
 - 19 Mamo JC, Smith D, Yu KC, Kawaguchi A, Harada-Shiba M, Yamamura T *et al*. Accumulation of chylomicron remnants in homozygous subjects with familial hypercholesterolaemia. *Eur J Clin Invest* 1998;28:379–84.
 - 20 Watts GF. Postprandial lipaemia in familial hypercholesterolemia: clinical and metabolic significance. *Atherosclerosis* 2000;148:426–8.
 - 21 Chan DC, Watts GF. Postprandial lipoprotein metabolism in familial hypercholesterolemia: thinking outside the box. *Metabolism* 2012;61:3–11.
 - 22 Tada H, Kawashiri MA, Noguchi T, Mori M, Tsuchida M, Takata M *et al*. A novel method for determining functional LDL receptor activity in familial hypercholesterolemia: application of the CD3/CD28 assay in lymphocytes. *Clin Chim Acta* 2009;400:42–7.
 - 23 Michaely P, Zhao Z, Li WP, Garuti R, Huang LJ, Hobbs HH *et al*. Identification of a VLDL-induced, FDNPVY independent internalization mechanism for the LDLR. *EMBO J* 2007;26:3273–82.

Arteriosclerosis, Thrombosis, and Vascular Biology



JOURNAL OF THE AMERICAN HEART ASSOCIATION

Liver-Specific Deletion of 3-Hydroxy-3-Methylglutaryl Coenzyme A Reductase Causes Hepatic Steatosis and Death

Shuichi Nagashima, Hiroaki Yagyu, Ken Ohashi, Fumiko Tazoe, Manabu Takahashi, Taichi Ohshiro, Tumenbayar Bayasgalan, Kenta Okada, Motohiro Sekiya, Jun-ichi Osuga and Shun Ishibashi

Arterioscler Thromb Vasc Biol. 2012;32:1824-1831; originally published online June 14, 2012;
doi: 10.1161/ATVBAHA.111.240754

Arteriosclerosis, Thrombosis, and Vascular Biology is published by the American Heart Association, 7272
Greenville Avenue, Dallas, TX 75231

Copyright © 2012 American Heart Association, Inc. All rights reserved.

Print ISSN: 1079-5642. Online ISSN: 1524-4636

The online version of this article, along with updated information and services, is located on the
World Wide Web at:

<http://atvb.ahajournals.org/content/32/8/1824>

Data Supplement (unedited) at:

<http://atvb.ahajournals.org/content/suppl/2012/06/14/ATVBAHA.111.240754.DC1.html>

Permissions: Requests for permissions to reproduce figures, tables, or portions of articles originally published in *Arteriosclerosis, Thrombosis, and Vascular Biology* can be obtained via RightsLink, a service of the Copyright Clearance Center, not the Editorial Office. Once the online version of the published article for which permission is being requested is located, click Request Permissions in the middle column of the Web page under Services. Further information about this process is available in the Permissions and Rights Question and Answer document.

Reprints: Information about reprints can be found online at:
<http://www.lww.com/reprints>

Subscriptions: Information about subscribing to *Arteriosclerosis, Thrombosis, and Vascular Biology* is online at:
<http://atvb.ahajournals.org/subscriptions/>

Liver-Specific Deletion of 3-Hydroxy-3-Methylglutaryl Coenzyme A Reductase Causes Hepatic Steatosis and Death

Shuichi Nagashima, Hiroaki Yagyu, Ken Ohashi, Fumiko Tazoe, Manabu Takahashi, Taichi Ohshiro, Tumenbayar Bayasgalan, Kenta Okada, Motohiro Sekiya, Jun-ichi Osuga, Shun Ishibashi

Objective—3-hydroxy-3-methylglutaryl coenzyme A reductase (HMGCR) catalyzes the rate-limiting step in cholesterol biosynthesis and has proven to be an effective target of lipid-lowering drugs, statins. The aim of this study was to understand the role of hepatic HMGCR in vivo.

Methods and Results—To disrupt the HMGCR gene in liver, we generated mice homozygous for a floxed HMGCR allele and heterozygous for a transgene encoding Cre recombinase under the control of the albumin promoter (liver-specific HMGCR knockout mice). Ninety-six percent of male and 71% of female mice died by 6 weeks of age, probably as a result of liver failure or hypoglycemia. At 5 weeks of age, liver-specific HMGCR knockout mice showed severe hepatic steatosis with apoptotic cells, hypercholesterolemia, and hypoglycemia. The hepatic steatosis and death were completely reversed by providing the animals with mevalonate, indicating its essential role in normal liver function. There was a modest decrease in hepatic cholesterol synthesis in liver-specific HMGCR knockout mice. Instead, they showed a robust increase in the fatty acid synthesis, independent of sterol regulatory element binding protein-1c.

Conclusion—Hepatocyte HMGCR is essential for the survival of mice, and its abrogation elicits hepatic steatosis with jaundice and hypoglycemia. (*Arterioscler Thromb Vasc Biol.* 2012;32:1824-1831.)

Key Words: cholesterol ■ liver ■ 3-hydroxy-3-methylglutaryl coenzyme A ■ fatty acids ■ knockout mouse

The mevalonate pathway produces isoprenoids that are essential for the diverse cellular functions ranging from cholesterol synthesis to growth control. The enzyme 3-hydroxy-3-methylglutaryl-coenzyme A reductase (HMGCR) (EC 1.1.1.34), which catalyzes the conversion of HMG-coenzyme A to mevalonate, is the rate-limiting enzyme in the mevalonate pathway.¹ Mammalian HMGCR is an integral high-mannose glycoprotein of the endoplasmic reticulum (ER).² Structurally, it is divided into 2 major domains: a C-terminal cytosolic-facing domain that tetramerizes to form the active site and an N-terminal hydrophobic region that spans the ER membrane 8× and bears a single N-glycan. This membrane region is dispensable for the enzymatic activity but necessary for the metabolically controlled stability of the enzyme and sufficient to cause sterol-accelerated degradation of heterologous proteins. Within this region, transmembrane spans 2 through 6 bear significant sequence homology to the corresponding transmembrane spans of sterol regulatory element binding protein (SREBP) cleavage-activating protein (SCAP).³

To ensure a steady supply of mevalonate, the nonsterol and sterol end products of the mevalonate metabolism exert feedback regulatory effects on the activity of this enzyme through multivalent mechanisms, including inhibition of the transcription of its RNA, blocking of translation, and acceleration of the

protein's degradation by a mechanism called ER-associated degradation, thereby regulating the amount of protein over a several hundred-fold range. ER-associated degradation of HMGCR requires the binding of Insig-1 to the sterol-sensing domain.⁴ Despite the critical role of HMGCR in cholesterol biosynthesis, little is known about its relevance to diseases. Only recently, HMGCR has been identified as a determinant of plasma cholesterol levels.⁵

Inhibitors of HMGCR, statins, are potent cholesterol-lowering agents that have been widely used to prevent the occurrence of coronary heart disease and other atherosclerotic diseases.⁶ The atheroprotective properties of statins are primarily because of the potent low-density lipoprotein (LDL)-cholesterol-lowering effect.⁷ Statins have also been reported to exert cholesterol-independent, or so-called pleiotropic, effects that involve improving endothelial function and decreasing oxidative stress and vascular inflammation.⁸ The benefits of statins extend beyond cardiovascular diseases and include a reduction in the risk of dementia, Alzheimer disease, ischemic stroke, osteoporosis, tumor growth, and viral infection. Most of these pleiotropic effects are mediated by an ability to block the synthesis of nonsterol isoprenoid intermediates. Statins have toxic effects in only a limited number of patients and are generally considered safe.

Received on: May 2, 2011; final version accepted on: April 30, 2012.

From the Division of Endocrinology and Metabolism, Department of Medicine, Jichi Medical University, Shimotsuke, Tochigi, Japan (S.N., H.Y., F.T., M.T., T.O., T.B., K. Okada, J.O., S.I.); and Department of Metabolic Diseases, Graduate School of Medicine, University of Tokyo, Tokyo, Japan (K. Ohashi, M.S.).

The online-only Data Supplement is available with this article at <http://atvb.ahajournals.org/lookup/suppl/doi:10.1161/ATVBAHA.111.240754/-DC1>. Correspondence to Shun Ishibashi, MD, PhD, Division of Endocrinology and Metabolism, Department of Medicine, Jichi Medical University, 3311-1 Yakushiji, Shimotsuke, Tochigi 329-0498, Japan. E-mail ishibash@jichi.ac.jp

© 2012 American Heart Association, Inc.

Arterioscler Thromb Vasc Biol is available at <http://atvb.ahajournals.org>

DOI: 10.1161/ATVBAHA.111.240754

Downloaded from <http://atvb.ahajournals.org/> at Jichi Medical School on February 20, 2013

To establish an animal model for investigating the mechanisms behind the effects, including toxicity of statins, we have generated HMGCR knockout (KO) mice lacking the enzyme throughout their bodies.⁹ These mice die in a relatively early stage of embryonic development (ie, before E8.5). Because mice lacking squalene synthase, the first committed enzyme in the sterol pathway, die in the embryonic stage with apparent anomalies of the development of the central nervous system,¹⁰ we took advantage of the tissue-specific gene targeting using the Cre-loxP system to generate mice lacking HMGCR in a liver-specific manner.

Materials and Methods

Liver-specific HMGCRKO (L-HMGCRKO) mice were generated by cross-breeding heterozygous floxed HMGCR (referred to as HMGCR^{f/f}; f denotes floxed) mice with transgenic mice expressing Cre recombinase under the control of albumin gene promoter (Alb-Cre).^{11,12} All animal experiments were performed with the approval of the Institutional Animal Care and Research Advisory Committee at Jichi Medical University. For detailed protocols for the generation of L-HMGCRKO mice and other experimental procedures, please refer to the online-only Data Supplement.

Results

Because there were no differences in growth curves or metabolic parameters, such as plasma lipid and glucose levels, among the HMGCR^{+/+} (wild-type), HMGCR^{f/+} Alb-Cre (CRE), and HMGCR^{f/f} (fHMGCR) mice, we used fHMGCR mice as a control. To determine whether the expression of the HMGCR gene was abrogated in the liver, we performed a Southern blot (Figure 1A), Northern blot (Figure 1B), and real-time polymerase chain reaction (Figure 1C). The Southern blot

analysis shows that only the 6.3-kb wild-type allele and 7.7-kb floxed allele were observed in the DNA from liver in wild-type and fHMGCR mice, respectively. In L-HMGCRKO mice at 3 weeks, the liver contained predominantly the 12.0-kb KO allele (70% based on PhosphorImager analysis [BAS 200, Fujifilm, Tokyo, Japan]) and some residual floxed allele (30%). The mRNA expression of HMGCR in the liver of L-HMGCRKO mice was decreased to 30% of the fHMGCR mice at 3 weeks of age and to <10% at 4 and 5 weeks upon Northern blot analysis. The time-dependent abrogation of the mRNA expression of HMGCR was also confirmed by real-time polymerase chain reaction. Based on this method, the mRNA levels were decreased to only 2% of the fHMGCR mice at 4 and 5 weeks, although there were no significant differences in other organs (Figure IIA in the online-only Data Supplement). Immunoblot analysis showed that the amount of HMGCR protein in the liver of L-HMGCRKO mice was 15% of that in fHMGCR mice (Figure 1D). Despite the profound reduction in HMGCR at both the mRNA and protein levels, the HMGCR activity in the liver of L-HMGCRKO mice was decreased by only 44% compared with that in fHMGCR mice (Figure 1E). To determine whether HMGCR is specifically abrogated in the liver parenchymal cells of L-HMGCRKO mice, we separated parenchymal and nonparenchymal cells from the liver at 3 weeks of age by density-gradient centrifugation after liver perfusion with collagenase. The mRNA expression of HMGCR in the parenchymal cells of L-HMGCRKO mice was decreased by 70.6% compared with that in fHMGCR mice, whereas the mRNA expression of HMGCR in the nonparenchymal cells was not different between the fHMGCR and L-HMGCRKO mice at 3 weeks of age (Figure IIC in the

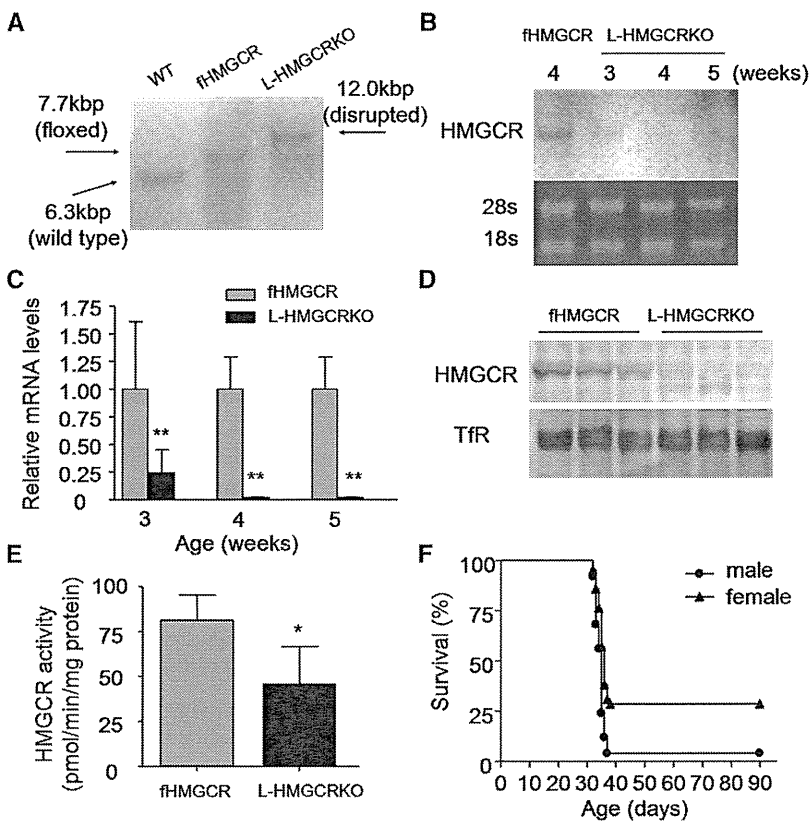


Figure 1. Conditional deletion of the 3-hydroxy-3-methylglutaryl-coenzyme A reductase (HMGCR) gene in mice and their survival. **A**, Southern blot analysis of *Bam*HI-digested DNA from the livers of wild-type (WT) floxed HMGCR (fHMGCR) and liver-specific HMGCR knockout (L-HMGCRKO) mice at 3 weeks of age as described in the online-only Data Supplement. **B**, Northern blot analysis of hepatic RNA from the livers of fHMGCR and L-HMGCRKO mice at 3, 4, and 5 weeks of age. Aliquots (20 µg) of total RNA from liver were subjected to electrophoresis and blot hybridization with ³²P-labeled cDNA probes for mouse HMGCR as described in the online-only Data Supplement. **C**, Quantitative real-time polymerase chain reaction of HMGCR mRNA levels from the livers of mice indicated in **B** (n=5 in each group). **D**, Immunoblot analysis of HMGCR protein from the livers of control and L-HMGCRKO mice at 4 weeks of age (n=3 in each group). Aliquots (50 µg) of liver membrane fractions were subjected to SDS-PAGE and immunoblot analysis. The membrane protein transferrin receptor was used as a loading control. **E**, HMGCR activity in the liver microsomal fractions of fHMGCR and L-HMGCRKO mice at 4 weeks of age (n=5 in each group). **F**, The survival curves were generated by the Kaplan-Meier method, and differences among the survival rates were compared using the χ^2 method. Male (n=25) and female (n=42) L-HMGCRKO mice were followed for >100 days. Each value represents mean±SD. Significant differences compared with control mice: *P<0.05 and **P<0.001.

Table. Liver Weight and Plasma Parameters of Control and L-HMGCRKO Mice

Age (wks)	3		4		5	
Genotype	fHMGCR (n=5)	L-HMGCRKO (n=5)	fHMGCR (n=9)	L-HMGCRKO (n=7)	fHMGCR (n=6)	L-HMGCRKO (n=5)
Body weight (g)	10.6±1.3	11.7±1.5	17.2±1.3	15.5±0.8*	21.7±2.0	13.5±0.8***
Liver weight (g)	0.47±0.11	0.51±0.11	0.78±0.14	0.92±0.13	1.08±0.11	1.17±0.28
Liver/body weight (%)	4.4±0.4	4.2±0.4	4.4±0.4	6.1±0.8*	5.0±0.12	8.7±2.1**
Total cholesterol (mg/dL)	63.6±9.1	47.1±1.0**	66.5±11.1	46.7±13.2**	64.6±6.8	282.6±72.6***
Free cholesterol (mg/dL)	26.2±4.0	20.1±0.5*	33.3±5.5	24.6±13.5	33.1±2.7	263.0±72.6***
Cholesterol ester (mg/dL)	37.4±5.5	27.0±1.4*	33.1±5.7	22.1±4.6*	31.5±4.9	19.6±10.3
Triglyceride (mg/dL)	62.5±13.3	51.1±9.9	78.5±25.4	24.9±6.9***	92.5±31.1	27.7±9.4**
Free fatty acids (mmol/L)	0.34±0.10	0.40±0.06	0.63±0.20	0.51±0.19	0.55±0.09	1.70±0.92*
Phospholipids (mg/dL)	132.2±20.2	106±2.7*	143.5±22.8	117.3±31.7	150.9±12.3	601.1±133.5**
Aspartate aminotransferase (IU/L)	76.1±10.2	95.7±45.5	92.7±39.3	343.1±602.8	55.9±18.6	1178.5±182.1***
Alanine transaminase (IU/L)	35.1±12.1	61.9±46.7	20.7±17.5	54.2±101.7	13.1±4.6	878.8±357.6**
Total bilirubin (mg/dL)	0.31±0.09	0.31±0.09	0.30±0.08	0.36±0.29	0.33±0.19	3.25±1.69*
Blood glucose (mg/dL)	110.6±16.7	123.0±15.5	115.9±13.7	99.6±16.7	135.7±9.4	48.3±23.3*

Blood samples were taken from male mice fed a normal chow diet ad libitum before the study. Each value represents the mean±SD. Significant differences compared with control mice: * $P<0.05$, ** $P<0.01$, and *** $P<0.001$. HMGCR indicates 3-hydroxy-3-methylglutaryl-coenzyme A reductase; L-HMGCRKO, liver-specific HMGCR knockout mice; fHMGCR, floxed HMGCR.

online-only Data Supplement). HMGCR activity in the parenchymal cells of L-HMGCRKO mice was decreased by only 47% compared with that in fHMGCR mice (Figure IID in the online-only Data Supplement). The relative decreases in the mRNA and activity of HMGCR in the parenchymal cells were similar to those observed in the whole liver of L-HMGCRKO mice (Figure 1C and E), supporting that HMGCR gene was specifically abrogated in the parenchymal cells of the liver and that there was no compensatory upregulation of HMGCR in the nonparenchymal cells of the L-HMGCRKO mice.

L-HMGCRKO mice were born at a rate in accordance with the rule of Mendelian inheritance. However, 96% of males died with a median survival time of 35 days, whereas 71% of females died with a median survival time of 36 days (Figure 1F), and the rest of them survived until 12 months of age. Therefore, the survival rate of females was significantly higher than males ($P=0.025$). The mRNA expression levels of HMGCR in the liver from the surviving HMGCRKO mice were as high as those from fHMGCR mice (Figure IIB in the online-only Data Supplement). Next, we compared body weight, liver weight, plasma lipid levels, liver functions, and blood glucose levels between fHMGCR and L-HMGCRKO mice (Table). Although the body weight of L-HMGCRKO mice was not different from that of fHMGCR mice at 3 weeks of age, it decreased by 10% at 4 weeks and by 38% at 5 weeks of age. Liver weight did not differ between the 2 groups. However, the ratio of liver weight to body weight was increased by 39% and 74% at 4 and 5 weeks of age, respectively. The livers of L-HMGCRKO mice were enlarged, paler, and whiter than those of fHMGCR mice at 5 weeks of age (Figure 2A and 2B). Consistent with the macroscopic abnormalities of the liver, plasma levels of aspartate aminotransferase, alanine transaminase, and bilirubin were markedly increased in the L-HMGCRKO mice compared with fHMGCR mice at 5 weeks of age. Total cholesterol levels in the plasma were decreased in the L-HMGCRKO mice by 26% at 3 weeks of age (Table). In parallel, plasma concentrations

of LDL cholesterol and apolipoprotein (apo) B-100 protein were decreased (Figure IIIA and IIIE in the online-only Data Supplement). Despite the liver failure of L-HMGCRKO mice at 5 weeks of age, the plasma levels of cholesterol, free cholesterol, and phospholipids were increased 4.3-, 7.9-, and 4.0-fold, respectively. On the other hand, plasma cholesterol ester levels were decreased by 38% (Table). Therefore, calculated ratios of free cholesterol to cholesterol ester were increased 13-fold. Most of the increased cholesterol was distributed in the size of very low-density lipoprotein through LDL (Figure IIIC in the online-only Data Supplement). Although apoB-100 levels were decreased, apoB-48 levels were substantially increased in the plasma of L-HMGCRKO mice at 5 weeks of age (Figure IIIG in the online-only Data Supplement). These findings together with the results of agar gel electrophoresis of the plasma (Figure III-I in the online-only Data Supplement) strongly indicate that both lipoprotein X and apoB-48-containing lipoproteins were increased in the L-HMGCRKO mice. Hepatic LDL receptor protein levels were not altered between fHMGCR and L-HMGCRKO mice at 3 and 5 weeks of age (Figure IIIF and IIHH in the online-only Data Supplement), despite increased hepatic LDL receptor mRNA levels (Figure 4A). Plasma lipoprotein changes in L-HMGCRKO mice may not be influenced by LDL receptor protein levels. Plasma free fatty acid levels were also increased 3.1-fold at 5 weeks. In contrast, plasma triglyceride levels were decreased by 69% and 70% at 4 and 5 weeks of age, respectively. It is of note that L-HMGCRKO mice were moderately hypoglycemic at 5 weeks.

To determine the causes of the liver dysfunction associated with hepatomegaly, we performed a microscopic analysis of the liver (Figure 2). Hematoxylin and eosin staining revealed moderate to severe ballooning and unicellular necrosis of parenchymal cells at 5 weeks (Figure 2C and 2D). Oil-red O staining showed moderate to severe microvesicular steatosis of the parenchymal cells (Figure 2E and 2F). TdT-mediated dUTP-nick end labeling–positive (Figure 2G, 2H, and 2M) and Ki-67–positive parenchymal cells

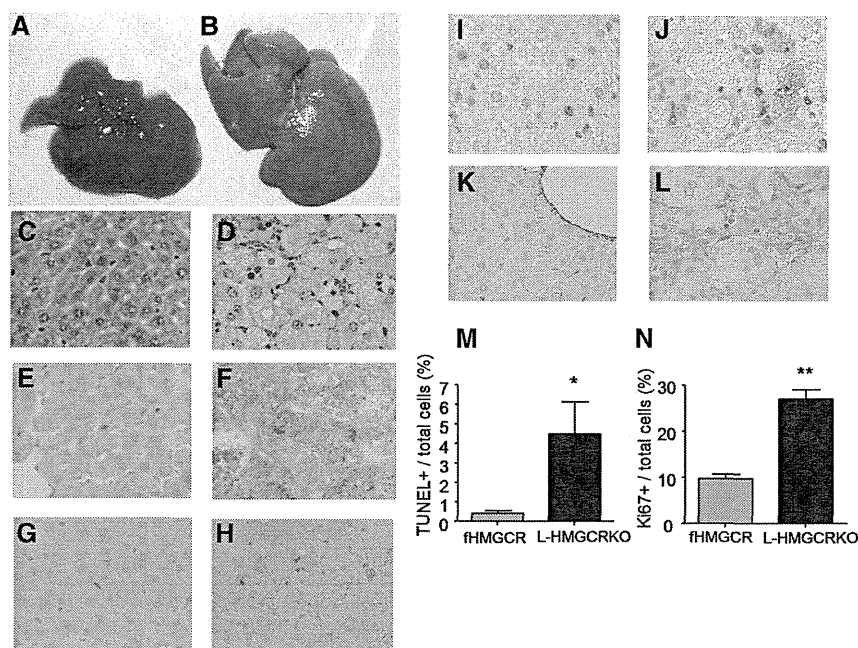


Figure 2. Gross appearance and histological analysis of the livers in male mice at 5 weeks. Gross appearance of the liver from control (A) and liver-specific HMGCR knockout (L-HMGCRKO) mice (B). Hematoxylin and eosin-stained liver sections from control (C) and L-HMGCRKO (D) mice. Frozen sections of liver stained with oil-red O from control (E) and L-HMGCRKO (F) mice. TdT-mediated dUTP-nick end labeling (TUNEL)-stained liver sections from control (G) and L-HMGCRKO (H) mice. Ki-67-stained liver sections from control (I) and L-HMGCRKO (J) mice. Type 4 collagen-stained liver sections from control (K) and L-HMGCRKO (L) mice. Bar graph shows the percentages of TUNEL-positive cells (M) and Ki-67-positive cells (N) relative to the total number of cells. Each value represents mean \pm SD. Significant differences compared with control mice: * $P < 0.01$ and ** $P < 0.001$.

(Figure 2I, 2J, and 2N) were significantly increased 11- and 2.8-fold in the liver of L-HMGCRKO mice compared with that in fHMGCR mice, respectively. The liver of L-HMGCRKO mice contained increased amounts of type 4 collagen (Figure 2K and 2L). Caspase 3 activity in the liver of L-HMGCRKO mice was also increased 1.8-fold compared with that of fHMGCR (Figure VA in the online-only Data Supplement). The mRNA levels of C/EBP-homologous protein were also significantly increased (Figure VD in the online-only Data Supplement). However, no significant differences were observed in either caspase 8 activity or H_2O_2 contents in the liver (Figure VB and VC in the online-only Data Supplement). The pathology of the liver from L-HMGCRKO mice at 4 weeks was milder (Figure IVB in the online-only Data Supplement) than that at 5 weeks. The liver of the mice which survived the lethal period still had hepatocyte ballooning (Figure IVD in the online-only Data Supplement).

To determine whether the liver-specific abrogation of HMGCR affected cholesterol metabolism in the liver, we measured the hepatic levels of cholesterol and triglycerides (Figure 3). The hepatic cholesterol content was decreased by only 22% in the L-HMGCRKO mice compared with the fHMGCR mice (Figure 3A). Unexpectedly, the hepatic contents of triglyceride were increased 2-fold (Figure 3B). These results indicate that the neutral lipids stained with oil-red O in the liver were primarily triglycerides. The reduction in the cholesterol contents of the liver was smaller than expected. We measured cholesterol synthesis in liver slices in culture (Figure 3C). The cholesterol synthesis was reduced by 45%. This reduction paralleled the degree of reduction in HMGCR activity in the liver (Figure 1E). We also measured the amounts of fatty acids synthesized in the liver (Figure 3D). Surprisingly, the synthesis of fatty acids from acetate was markedly increased 17-fold in the liver of L-HMGCRKO mice. Although total amounts of fatty acids were not different between the 2 mice (Figure 3E), the following fatty acid species were significantly increased in the liver of L-HMGCRKO mice: C18:0, C18:1n-9, C20:1n-9,

C20:3n-9, and C22:4n-6 (Figure 3F). Given the increased production of fatty acids and triglycerides in the liver, we measured other metabolites of fatty acids such as diglycerides and ceramides. The hepatic levels of diglycerides were increased 1.8-fold (Figure 3G), but those of ceramides were not increased significantly (Figure 3H).

To clarify the mechanisms behind the changes in fatty acid metabolism, we determined the changes in the levels of mRNA expression in various genes involved in cholesterol or fatty acid metabolism in the liver at 4 weeks of age by real-time polymerase chain reaction (Figure 4A). As to the genes involved in cholesterol metabolism, the mRNA levels of SREBP2, LDL receptor, proprotein convertase subtilisin/kexin type 9, and squalene synthase were increased 1.4-, 1.9-, 2.8-, and 3.9-fold, respectively. On the other hand, the mRNA levels of cholesterol 7 α -hydroxylase, a rate-limiting enzyme for bile acid synthesis, were decreased by 60%. With regard to the genes involved in fatty acid metabolism, the mRNA levels of fatty acid synthase (FAS), acetyl-CoA carboxylase, and stearoyl-CoA desaturase 2 were increased 2.4-, 1.4-, and 22-fold, respectively. On the other hand, the mRNA expression of SREBP1c and acyl CoA:diacylglycerol acyltransferase 2 was decreased by 80% and 40%, respectively. There were no changes in either the mRNA expression of SREBP1a, a splice variant of SREBP1c, or liver X receptor α (LXR α), an important transcriptional activator of the SREBP1c gene. The mRNA expression of peroxisome proliferator-activated receptor α , a transcription regulator of genes for fatty acid oxidation, was not changed.

HMGCR catalyzes the formation of mevalonate, which is used as a substrate for the synthesis not only of cholesterol but also nonsterols such as isoprenoids, ubiquinone, heme A, and dolichol. To test the notion that death, likely because of severe liver failure, was caused by the alteration of a nonsterol pathway, we evaluated the isoprenylation of small GTP-binding proteins such as H-Ras and Rac1 by measuring the amount of membrane-bound forms (Figure 4B). The ratio of the

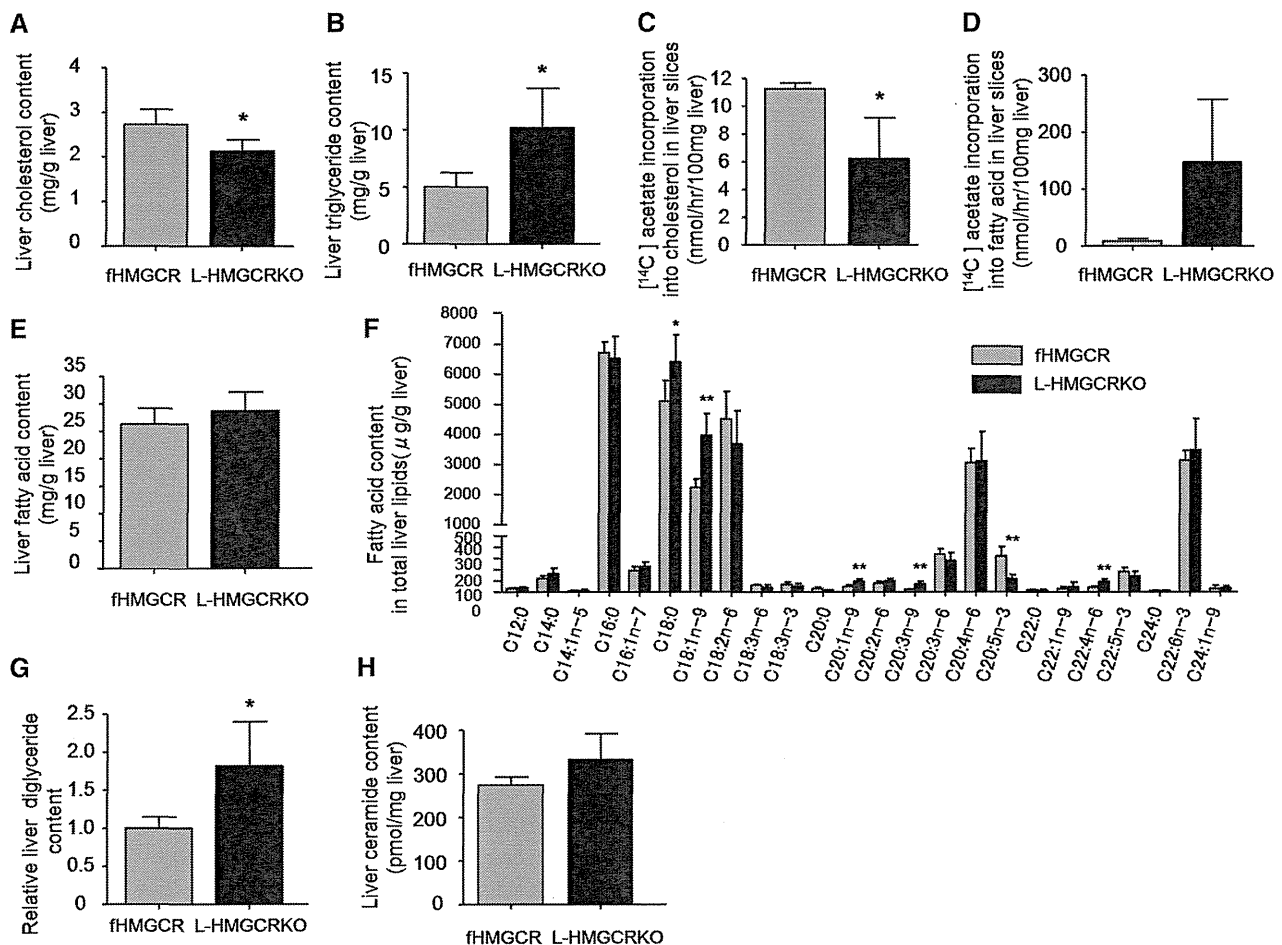


Figure 3. Hepatic lipid contents and lipid synthesis in the control and liver-specific HMGR knockout (L-HMGCRKO) male mice. Hepatic total cholesterol (A), triglyceride (B), fatty acid levels (E), and fatty acid composition in total liver lipids (F) were determined in the livers from control and L-HMGCRKO mice at 4 weeks of age (n=5 in each group). C and D, In vitro hepatic lipid synthesis rate using the liver slices in culture (n=3 in control and n=4 in L-HMGCRKO). Liver slices (≈ 100 mg) were incubated with ^{14}C -labeled acetate (8 mmol/L, 0.1 $\mu\text{Ci}/\mu\text{mol}$) for 90 minutes. After incubation, the slices were removed for measurement of ^{14}C -labeled cholesterol (C) and fatty acids (D). Hepatic diglyceride (G) and ceramide (H) contents were measured in the livers of control and L-HMGCRKO mice at 4 weeks of age (n=5 in each group) by the diglyceride kinase method as described in the online-only Data Supplement. Each value represents mean \pm SD. Significant differences compared with control mice: * $P < 0.05$ and ** $P < 0.01$.

membrane-bound form to the cytosolic form of H-Ras or Rac1 was decreased to 0.05 to 0.2 compared with control. These results indicate that the deficiency of HMGR affected the nonsterol pathway more severely than the sterol pathway. We also estimated changes in intracellular signaling molecules (Figure 4C). p-Akt and c-Met were decreased by 72% and 81%, respectively, whereas phospho-signal transducer and activator of transcription 3 was increased 7.6-fold.

If the lethal phenotype of HMGR deficiency is because of the deficiency of mevalonate, supplementation with mevalonate could theoretically rescue the lethal phenotype. In fact, providing the male mice with water containing mevalonate significantly attenuated the liver dysfunction and hypercholesterolemia (Figure 5A–5C). The pathological abnormalities observed in the male L-HMGCRKO mice were almost normalized by the supplementation with mevalonate (Figure 5D–5G). Consistently, the amounts of the membrane-bound form of H-Ras or Rac 1 were restored to normal levels (Figure 5H). Similar improvements were found in female L-HMGCRKO

mice (data not shown). No death occurred until 40 days of age in L-HMGCRKO mice supplemented with mevalonate.

Because L-HMGCRKO mice were hypoglycemic (Table), it is possible that hypoglycemia is the direct cause of death. To test this hypothesis, we allowed mice free access to drinking water containing 20% (w/v) glucose. Glucose feeding significantly increased plasma glucose levels (43.5 ± 16.2 mg/dL [n=10] versus 79.5 ± 40.6 mg/dL [n=13] [$P=0.01$] in males; 36.6 ± 13.3 mg/dL [n=4] versus 65.2 ± 35.6 mg/dL [n=11] [$P=0.04$] in females). Concurrently, it dramatically improved the mortality of L-HMGCRKO mice (96% versus 13% in males and 71% versus 15% in females) (Figure VI in the online-only Data Supplement).

Discussion

Nearly all the male L-HMGCRKO mice died before 40 days of age, whereas 30% of females survived until 12 months of age. Before their death, the mice developed severe hepatic damage with hepatomegaly, steatosis, and hypoglycemia. Thus, we ascribe the lethal effect of the liver-specific deficiency of HMGR

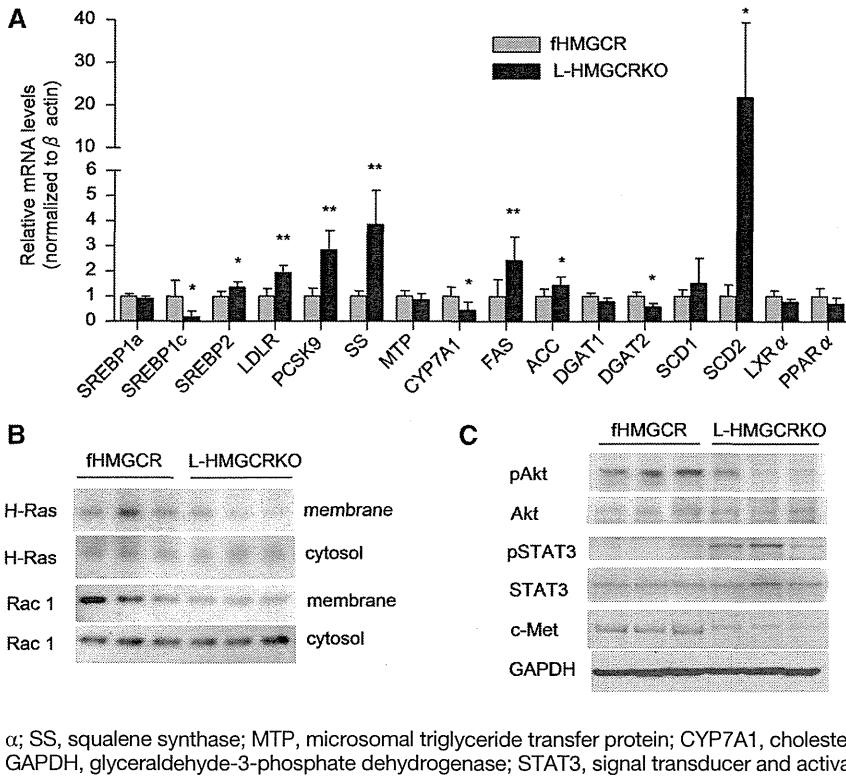


Figure 4. Relative amounts of various mRNAs and degree of isoprenylation of small GTP-binding proteins and liver regeneration-associated proteins in the livers of control and liver-specific HMGCR knockout (L-HMGCRKO) male mice at 4 weeks of age. **A**, Total RNA from the livers of mice (n=5 in each group) was subjected to quantitative real-time polymerase chain reaction as described in the online-only Data Supplement. Each value represents the amount of mRNA relative to that in the control mice, which is arbitrarily defined as 1. **B**, Liver membranous and cytosolic fractions for small GTP-binding proteins or **(C)** liver tissue lysates for liver regeneration-associated proteins were prepared as described in the online-only Data Supplement (n=3 in each group), and aliquots (30 μ g) were subjected to SDS-PAGE and immunoblot analysis. Each value represents mean \pm SD. Significant differences compared with control mice: * P <0.05 and ** P <0.01. LDLR indicates low-density lipoprotein receptor; PCSK9, proprotein convertase subtilisin/kexin type 9; FAS, fatty acid synthase; DGAT, diacylglycerol acyltransferase; SCD, stearyl-CoA desaturase; LXR α , liver X receptor; PPAR α , peroxisome proliferator-activated receptor

α ; SS, squalene synthase; MTP, microsomal triglyceride transfer protein; CYP7A1, cholesterol 7 α -hydroxylase; ACC, acetyl-CoA carboxylase; GAPDH, glyceraldehyde-3-phosphate dehydrogenase; STAT3, signal transducer and activator of transcription 3.

to the hepatic toxicity and hypoglycemia. Unexpectedly, the mice developed hypercholesterolemia before death, although hepatic cholesterol synthesis was significantly reduced. This lethal phenotype was completely reversed by mevalonate or glucose, indicating that mevalonate is essential for the survival of mice and that hypoglycemia is the direct cause of lethality.

The mRNA expression of HMGCR was reduced as early as 3 weeks of age and almost undetectable at 4 weeks. This developmental reduction in the expression is consistent with the developmental induction of the expression of albumin. Other

liver-specific KO models using Alb-Cre showed abrogation of the expression of reporter genes at a similar stage.¹² However, the HMGCR activity of the liver was reduced by only 50%. Because the parenchymal hepatocytes from the liver of the L-HMGCRKO mice at 3 weeks of age expressed substantial HMGCR activity, we speculate that most of the activity is derived from upregulated HMGCR expression in a certain subset of hepatocytes that escaped from HMGCR gene inactivation. Indeed, recombination efficiency was only 75% at weaning,¹³ and HMGCR protein can be increased 25-fold at the posttranscriptional level.¹

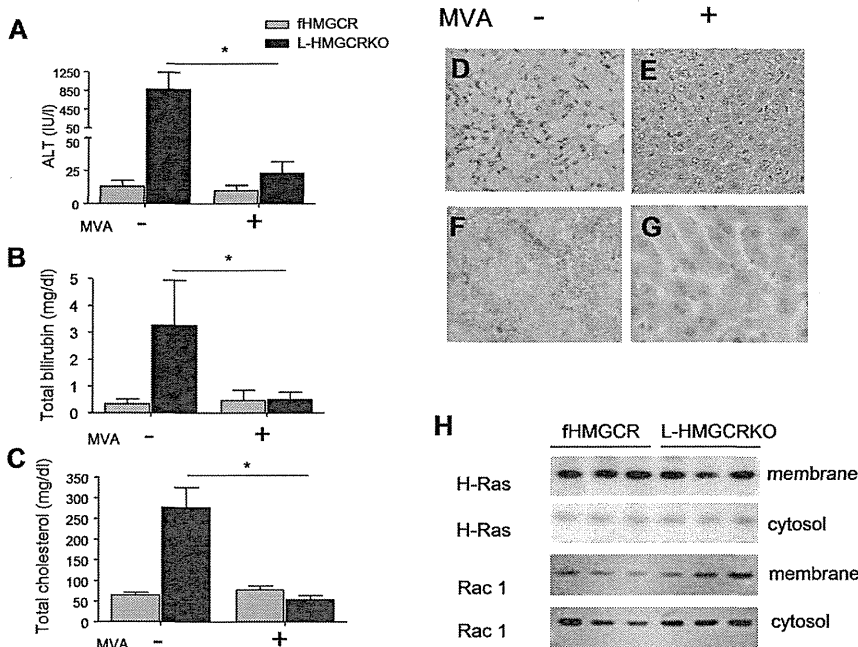


Figure 5. Supplementation of mevalonate. Male mice were given mevalonate in drinking water at a concentration of 5 mmol/L from the age of 28 days to 35 days (n=5 in each group). After supplementation, plasma alanine transaminase (ALT) **(A)**, total bilirubin **(B)**, and total cholesterol **(C)** levels were measured. The livers were removed from liver-specific HMGCR knockout (L-HMGCRKO) mice not supplemented with mevalonate (**-**; **D** and **F**, respectively) or supplemented with mevalonate (**+**; **E** and **G**, respectively) stained with hematoxylin and eosin or oil-red O. **H**, Immunoblot analyses for small GTP-binding proteins in membranous and cytosolic fractions of the liver. Each value represents mean \pm SD. Significant differences compared with control mice: * P <0.001.

Furthermore, there might be time lag between disappearance of HMGCR protein and cessation of transcription.

Sex dimorphism in lethality is noteworthy. The present results that male L-HMGCRKO mice were more prone to die than females are consistent with the general view that females are more resistant to morbidity and mortality of various liver diseases than males.¹⁴ In addition to protection against liver injury via vasodilating and anti-inflammatory effects, estrogen itself attenuates the development of hepatic steatosis.¹⁵ The mRNA expression levels of HMGCR in the liver of the surviving L-HMGCRKO mice were indistinguishable from those of fHMGCR mice (Figure IIB in the online-only Data Supplement). It is likely that the hepatocytes with a relatively intact HMGCR gene may be extensively regenerated, thereby eventually compensating for the KO in the survivors. In support of this, several Ki-67-positive cells were greatly increased in the L-HMGCRKO mice (Figure 2L and 2N).

Hepatic cholesterol levels were mildly decreased, and the decrease in plasma cholesterol levels was modest in the L-HMGCRKO mice at 3 weeks of age. More surprisingly, the plasma cholesterol levels even increased immediately before death. Extrahepatic organs with high cholesterol synthesis, such as skin, bowels, and muscles, may be a source of cholesterol in the plasma.¹⁶ The hypercholesterolemia before death appears paradoxical, given the failure of cholesterol synthesis in the hepatocytes. At this stage, the mice develop jaundice. Because the physicochemical characteristics of the accumulated lipoproteins were similar to those of lipoprotein X, cholestasis may at least partly account for hypercholesterolemia. Simultaneous accumulation of both lipoprotein X and apoB48-containing particles has also been reported in rats with intrahepatic cholestasis.¹⁷

Interestingly, L-HMGCRKO mice showed hepatic steatosis. Because hepatic triglyceride levels were increased 2-fold but hepatic cholesterol ester levels were not increased (data not shown) most of the neutral lipids stained with oil-red O are triglycerides. Supporting this, the synthesis of fatty acids was increased 17-fold. In this context, it is noteworthy that the expression of enzymes for fatty acid synthesis, FAS and stearoyl-CoA desaturase 2, was increased. In normal adults, stearoyl-CoA desaturase 1 is the major enzyme catalyzing desaturation of oleate, whereas stearoyl-CoA desaturase 2 is an isozyme that is transiently expressed in the liver in embryos and neonates and may be involved in lipogenesis at that developmental stage.¹⁸ Indeed, the amounts of polyunsaturated fatty acids were increased in the liver (Figure 3F).

The increase in fatty acids synthesis appeared disproportionately larger than the increase in triglycerides in the liver. In this context, it is of note that the expression of diacylglycerol acyltransferase 1 was not increased and that of diacylglycerol acyltransferase 2 was even decreased. Thus, it is probable that the newly synthesized fatty acids were not used to produce triglycerides. Generally, the enzymes catalyzing fatty acid synthesis are transcriptionally induced by SREBP1c. However, the expression of SREBP1c was reduced 5-fold, suggesting that the increased lipogenesis was not mediated by SREBP1c. Similar SREBP1c-independent lipogenesis is reported in mice overexpressing a constitutively active form of Akt in the liver.¹⁹ Furthermore, the levels of LXR α mRNA, a nuclear receptor that can stimulate SREBP1c gene expression²⁰ and can also directly

stimulate transcription of FAS,²¹ were not increased in the livers of L-HMGCRKO mice. We speculate that the lack of cholesterol reduces the supply of oxysterols, physiological ligands of LXR, which transactivates SREBP1c.²² This notion is supported by the decreased expression of cholesterol 7 α -hydroxylase and diacylglycerol acyltransferase 2, also targets of LXR.

In contrast to SREBP1c expression, the expression of SREBP2 was increased, conceivably accounting for the increased expression of its targets: the LDL receptor and squalene synthase. The expression of FAS in the face of significant suppression of SREBP1c or unaltered LXR α suggests a regulatory pathway independent of SREBP1c or LXR α . Recently, a decrease in farnesyl pyrophosphate or farnesol has been shown to induce the expression of FAS independently of SREBP1c.²³

The liver of the L-HMGCRKO mice contained increased numbers of TdT-mediated dUTP-nick end labeling-positive cells. Consistent with the apoptotic nature of the cell death, the activity of caspase 3, a final executor of apoptosis which cleaves to induce the release of cytochrome c from mitochondria, was increased in the liver of the L-HMGCRKO mice. We have hypothesized several potential mechanisms for apoptosis: accumulation of toxic lipid metabolites²⁴ and reduction of survival factors.²⁵ However, we failed to obtain evidence for the involvement of ceramide and survivin in apoptosis.

As predicted, membrane-bound forms of Ras and Rac1 were significantly reduced, conceivably as a result of the defect in their isoprenylation. Several mechanisms linking the defect in isoprenylation to apoptosis have been proposed. For example, Rac1 is reported to protect against apoptosis by stimulating nicotinamide adenine dinucleotide phosphate-oxidase, thereby increasing the levels of reactive oxygen species.²⁶ However, we failed to detect a decrease in H₂O₂ levels in the liver.

During the search for the plausible mechanism of the hepatocyte apoptosis, we found a significant increase in the mRNA level of C/EBP-homologous protein, a hallmark of the ER stress response and inducer of apoptosis, in the liver of L-HMGCRKO mice. Because hepatic steatosis induces ER stress, it is reasonable to speculate that the increased synthesis of fatty acids causes hepatic lipoapoptosis via increasing the C/EBP-homologous protein. The liver of L-HMGCRKO mice had significantly decreased levels of either p-Akt or c-met protein. Because hepatocyte growth factor exerts pro-survival effects mainly through activating phosphatidylinositol-3 kinase/Akt pathway after binding to its receptor, c-met,²⁷ defective hepatocyte growth factor signaling may play a salutary role in the induction of hepatocyte apoptosis. The increase in phospho-signal transducer and activator of transcription 3 might be a compensatory response secondary to increased apoptosis, but failed to overcome it. Similar failure to compensate the liver failure by activated signal transducer and activator of transcription 3 was reported in mice deficient in phosphoinositide-dependent protein kinase 1.²⁸

These phenotypes of L-HMGCRKO mice should be discussed in relation to other mouse models of genetic disorders of cholesterol metabolism. Thus far, 2 models have been reported to survive the perinatal period, despite reduced cholesterol biosynthesis in the liver. Because the global disruption of SREBP cleavage-activating protein and site 1 protease is embryonic lethal, as is the case for HMGCR, liver-specific KO

mice have been generated. In both the liver-specific SREBP cleavage-activating protein²⁹ and site 1 protease KO mice,³⁰ the synthesis of cholesterol as well as fatty acids was significantly reduced in the liver. Neither mouse, however, died of liver toxicity, probably because the reduction in the expression of HMGR was not as severe as in L-HMGRKO mice.

In conclusion, HMGR is essential for the survival of mice. Despite the defect in hepatic cholesterol biosynthesis in L-HMGRKO mice, the homeostasis of cholesterol in the liver and plasma is surprisingly well maintained presumably via compensatory changes in the flux of cholesterol and fatty acids. These results might provide insight for understanding the role of cholesterol biosynthetic pathway in the normal function of hepatocytes.

Acknowledgments

We thank Drs Derek LeRoith, Wataru Ogawa, and Masato Kasuga for providing Alb-Cre mice. We also thank Drs Tetsuya Kitamine, Ryuichi Tozawa, Yoshiaki Tamura, Hiroaki Okazaki, Masaki Igarashi, Hitoshi Shimano, and Nobuhiro Yamada for their help and discussion.

Sources of Funding

This work was supported by a Grant-in-Aid for Scientific Research from the Ministry of Education, Science and Culture and the Program for Promotion of Fundamental Studies in Health Sciences of the National Institute of Biomedical Innovation (NIBIO) and JKA through its promotion funds from KEIRIN RACE.

Disclosures

None.

References

- Goldstein JL, Brown MS. Regulation of the mevalonate pathway. *Nature*. 1990;343:425–430.
- Liscum L, Finer-Moore J, Stroud RM, Luskey KL, Brown MS, Goldstein JL. Domain structure of 3-hydroxy-3-methylglutaryl coenzyme A reductase, a glycoprotein of the endoplasmic reticulum. *J Biol Chem*. 1985;260:522–530.
- Hua X, Nohturfft A, Goldstein JL, Brown MS. Sterol resistance in CHO cells traced to point mutation in SREBP cleavage-activating protein. *Cell*. 1996;87:415–426.
- Sever N, Yang T, Brown MS, Goldstein JL, DeBose-Boyd RA. Accelerated degradation of HMG CoA reductase mediated by binding of insig-1 to its sterol-sensing domain. *Mol Cell*. 2003;11:25–33.
- Kathiresan S, Melander O, Guiducci C, Surti A, Burt NP, Rieder MJ, Cooper GM, Roos C, Voight BF, Havulinna AS, Wahlstrand B, Hedner T, Corella D, Tai ES, Ordovas JM, Berglund G, Vartiainen E, Jousilahti P, Hedblad B, Taskinen MR, Newton-Cheh C, Salomaa V, Peltonen L, Groop L, Altshuler DM, Orho-Melander M. Six new loci associated with blood low-density lipoprotein cholesterol, high-density lipoprotein cholesterol or triglycerides in humans. *Nat Genet*. 2008;40:189–197.
- Endo A, Kuroda M, Tanzawa K. Competitive inhibition of 3-hydroxy-3-methylglutaryl coenzyme A reductase by ML-236A and ML-236B fungal metabolites, having hypocholesterolemic activity. *FEBS Lett*. 1976;72:323–326.
- Baigent C, Keech A, Kearney PM, Blackwell L, Buck G, Pollicino C, Kirby A, Sourjina T, Peto R, Collins R, Simes R; Cholesterol Treatment Trialists' (CTT) Collaborators. Efficacy and safety of cholesterol-lowering treatment: prospective meta-analysis of data from 90,056 participants in 14 randomised trials of statins. *Lancet*. 2005;366:1267–1278.
- Liao JK, Laufs U. Pleiotropic effects of statins. *Annu Rev Pharmacol Toxicol*. 2005;45:89–118.
- Ohashi K, Osuga J, Tozawa R, Kitamine T, Yagyu H, Sekiya M, Tomita S, Okazaki H, Tamura Y, Yahagi N, Iizuka Y, Harada K, Gotoda T, Shimano H, Yamada N, Ishibashi S. Early embryonic lethality caused by targeted disruption of the 3-hydroxy-3-methylglutaryl-CoA reductase gene. *J Biol Chem*. 2003;278:42936–42941.
- Tozawa R, Ishibashi S, Osuga J, Yagyu H, Oka T, Chen Z, Ohashi K, Perrey S, Shionoiri F, Yahagi N, Harada K, Gotoda T, Yazaki Y, Yamada N. Embryonic lethality and defective neural tube closure in mice lacking squalene synthase. *J Biol Chem*. 1999;274:30843–30848.
- Yakar S, Liu JL, Stannard B, Butler A, Accilli D, Sauer B, LeRoith D. Normal growth and development in the absence of hepatic insulin-like growth factor I. *Proc Natl Acad Sci USA*. 1999;96:7324–7329.
- Inoue H, Ogawa W, Ozaki M, Haga S, Matsumoto M, Furukawa K, Hashimoto N, Kido Y, Mori T, Sakaue H, Teshigawara K, Jin S, Iguchi H, Hiramatsu R, LeRoith D, Takeda K, Akira S, Kasuga M. Role of STAT-3 in regulation of hepatic gluconeogenic genes and carbohydrate metabolism in vivo. *Nat Med*. 2004;10:168–174.
- Postic C, Magnuson MA. DNA excision in liver by an albumin-Cre transgene occurs progressively with age. *Genesis*. 2000;26:149–150.
- Yokoyama Y, Nimura Y, Nagino M, Bland KI, Chaudry IH. Current understanding of gender dimorphism in hepatic pathophysiology. *J Surg Res*. 2005;128:147–156.
- Nemoto Y, Toda K, Ono M, Fujikawa-Adachi K, Saibara T, Onishi S, Enzan H, Okada T, Shizuta Y. Altered expression of fatty acid-metabolizing enzymes in aromatase-deficient mice. *J Clin Invest*. 2000;105:1819–1825.
- Spady DK, Dietschy JM. Sterol synthesis in vivo in 18 tissues of the squirrel monkey, guinea pig, rabbit, hamster, and rat. *J Lipid Res*. 1983;24:303–315.
- Chisholm JW, Dolphin PJ. Abnormal lipoproteins in the ANIT-treated rat: a transient and reversible animal model of intrahepatic cholestasis. *J Lipid Res*. 1996;37:1086–1098.
- Miyazaki M, Dobrzyn A, Elias PM, Ntambi JM. Stearoyl-CoA desaturase-2 gene expression is required for lipid synthesis during early skin and liver development. *Proc Natl Acad Sci USA*. 2005;102:12501–12506.
- Ono H, Shimano H, Katagiri H, Yahagi N, Sakoda H, Onishi Y, Anai M, Ogihara T, Fujishiro M, Viana AY, Fukushima Y, Abe M, Shojima N, Kikuchi M, Yamada N, Oka Y, Asano T. Hepatic Akt activation induces marked hypoglycemia, hepatomegaly, and hypertriglyceridemia with sterol regulatory element binding protein involvement. *Diabetes*. 2003;52:2905–2913.
- Chen G, Liang G, Ou J, Goldstein JL, Brown MS. Central role for liver X receptor in insulin-mediated activation of Srebp-1c transcription and stimulation of fatty acid synthesis in liver. *Proc Natl Acad Sci USA*. 2004;101:11245–11250.
- Joseph SB, Laffitte BA, Patel PH, Watson MA, Matsukuma KE, Walczak R, Collins JL, Osborne TF, Tontonoz P. Direct and indirect mechanisms for regulation of fatty acid synthase gene expression by liver X receptors. *J Biol Chem*. 2002;277:11019–11025.
- Yoshikawa T, Shimano H, Amemiya-Kudo M, Yahagi N, Hasty AH, Matsuzaka T, Okazaki H, Tamura Y, Iizuka Y, Ohashi K, Osuga J, Harada K, Gotoda T, Kimura S, Ishibashi S, Yamada N. Identification of liver X receptor-retinoid X receptor as an activator of the sterol regulatory element-binding protein 1c gene promoter. *Mol Cell Biol*. 2001;21:2991–3000.
- Murthy S, Tong H, Hohl RJ. Regulation of fatty acid synthesis by farnesyl pyrophosphate. *J Biol Chem*. 2005;280:41793–41804.
- Anderson N, Borlak J. Molecular mechanisms and therapeutic targets in steatosis and steatohepatitis. *Pharmacol Rev*. 2008;60:311–357.
- Kaneko R, Tsuji N, Asanuma K, Tanabe H, Kobayashi D, Watanabe N. Survivin down-regulation plays a crucial role in 3-hydroxy-3-methylglutaryl coenzyme A reductase inhibitor-induced apoptosis in cancer. *J Biol Chem*. 2007;282:19273–19281.
- Deshpande SS, Angekov P, Huang J, Ozaki M, Irani K. Rac1 inhibits TNF-alpha-induced endothelial cell apoptosis: dual regulation by reactive oxygen species. *FASEB J*. 2000;14:1705–1714.
- Xiao GH, Jeffers M, Bellacosa A, Mitsuchi Y, Vande Woude GF, Testa JR. Anti-apoptotic signaling by hepatocyte growth factor/Met via the phosphatidylinositol 3-kinase/Akt and mitogen-activated protein kinase pathways. *Proc Natl Acad Sci USA*. 2001;98:247–252.
- Haga S, Ozaki M, Inoue H, Okamoto Y, Ogawa W, Takeda K, Akira S, Todo S. The survival pathways phosphatidylinositol-3 kinase (PI3-K)/phosphoinositide-dependent protein kinase 1 (PDK1)/Akt modulate liver regeneration through hepatocyte size rather than proliferation. *Hepatology*. 2009;49:204–214.
- Matsuda M, Korn BS, Hammer RE, Moon YA, Komuro R, Horton JD, Goldstein JL, Brown MS, Shimomura I. SREBP cleavage-activating protein (SCAP) is required for increased lipid synthesis in liver induced by cholesterol deprivation and insulin elevation. *Genes Dev*. 2001;15:1206–1216.
- Yang J, Goldstein JL, Hammer RE, Moon YA, Brown MS, Horton JD. Decreased lipid synthesis in livers of mice with disrupted Site-1 protease gene. *Proc Natl Acad Sci USA*. 2001;98:13607–13612.